SYNTHESIS AND EVALUATION OF THE SIGMA RECEPTORS LIGAND 4-((4-[123]I]IODOPHENOXY)METHYL)-1-(2-FLUOROETHYL)PIPERIDINE IN ANIMAL TUMOUR MODELS

A. Katsifis,[1] F. Mattner,[1] T. Pham,[1] X. Liu,[1] P. Berghofer,[1] I. Greguric,[1] P. Ballantyne,[1] J. Chapman,[1] V. Nguyen,[1] T. Homes,[2] P. Keller,[2] L. Berwick,[1] V. Papazian,[1] T. Jackson,[1] R. Waterhouse,[3] C. Loc'h.[1]

[1]Radiopharmaceuticals Research Institute, ANSTO, Sydney, NSW, Australia; [2]Department of Chemistry, Wolongong University, Wolongong, NSW, Australia; [3]Department of Psychiatry, Columbia University, New York, NY, United States.

Introduction: Because of their potential role in various biochemical and physiological processes, sigma receptors have been the target of extensive research studies. In addition to their role in several CNS disorders, enhanced sigma receptor expression has also been observed in a number of tumours. Recently a series of substituted aryloxy piperidines have been reported as high affinity ligands for the sigma-1 receptor. Furthermore these compounds have been radiolabelled with both iodine-123 and fluorine-18. Based on these lead compounds, we have synthesised several iodinated and fluorinated analogues which would serve as radioligands for use in PET and SPECT. Here we report the synthesis, and *in vivo* evaluation of [^{123}I]-4-((4-iodophenoxy)methyl)-1-(2-fluoroethyl)piperidine [^{123}I]**1** in B-16 and A375 melanoma tumours as well as in rat mammary adenocarcinomas.

Methods: [^{123}I]**1** was prepared by [^{123}I]iododestannylation of the corresponding tributyl stannane derivative in ethanol using chloramine-T as oxidant. The biodistribution of [^{123}I]**1** was undertaken in B16 and A375 mouse melanoma tumour models as well as in Fisher rats bearing mammary adenocarcinoma and analysis up to 24 h p.i. *In vivo* imaging of [^{123}I]**1** was performed on an X-SPECT scanner in all three animal models. Pre-treatment with sigma specific ligands (1 mg/kg) 5 min prior to injection was carried out in all of the above studies.

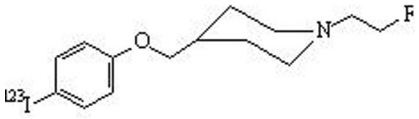

Results: *In vitro* binding revealed that **1** is a selective σ_1 ligand (Ki σ_1 = 0.84 nM, σ_2 = 102 nM). [^{123}I]**1** was synthesised in 73-85% radiochemical yield and >98% radiochemical purity. The *in vivo* biodistribution of [^{123}I]**1** in both the B-16 and A375 tumoured mice showed high uptake in the tumour (4 and 2% ID/g respectively) as early as 60 min and peaking at 24h (11 and 4% ID/g). High uptake was also observed in the mouse brain 9 and 7.5% ID/g at 60 min for B16 and A375 but with rapid clearance. Pre-treatment of mice with haloperidol (1 mg/kg) reduced radioligand uptake by 40% in brain at 1h and 70% in brain and tumour at 24 h. A high uptake of activity was also observed in the mammary tumour (0.55% ID/g at 1h and plateau till 6h and at 24 h 0.47% ID/g). High uptake was also observed in the rat brain 2.20 %ID/g at 60 min but with rapid clearance. Imaging studies of [^{123}I]**1** in both mice and rats indicated high uptake in tumour tissue with rapid clearance from other organs.

Conclusion: These results demonstrate the specific sigma receptor uptake of [^{123}I]**1** in tumours *in vivo* and could be further developed as a SPECT imaging agent in oncology. The radiolabelling of **1** with F-18 is in progress.

Keywords: sigma Receptor, SPECT, Tumours

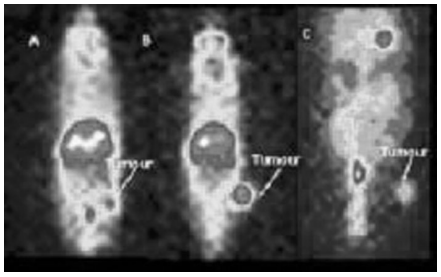

EVALUATION OF [*N*-METHYL-^{11}C]PK 11195 FOR DETECTION OF BREAST CANCER

S.E. Shockley, S.M. Moerlein, S.G. Adams, M.J. Welch.
The Edward Mallinckrodt Institute of Radiology, Washington University School of Medicine, Saint Louis, MO, United States.

[*N*-methyl-^{11}C]PK 11195 ([^{11}C]PK) is a peripheral benzodiazepine receptor (PBR) ligand used as a tracer for PET imaging of the brain. One of its applications is detection of brain tumors that express PBR. We are interested in evaluating [^{11}C]PK for the detection of PBR-expressing tumors outside of the central nervous system.

There is a positive relationship between proliferation rates and PBR expression in human breast cancer lines (*1, 2*). In order to evaluate the potential of [^{11}C]PK to image tumor and tumor proliferation, studies were conducted *in vitro* and *in vivo*. The *in vitro* uptake of [^{11}C]PK was measured in cell lines displaying a wide range of PBR expression. Biodistribution studies were conducted in female tumor-bearing nude mice to assess the ability of [^{11}C]PK to localize to tumor.

[^{11}C]PK is synthesized via N-methylation of (R)-*N*-desmethyl PK 11195 (from ABX GmbH, Radeberg, FRG) using [^{11}C]CH_3I produced with a PETtrace MeI Microlab. Product was purified by reverse phase preparative HPLC, and reformulated in 10% ethanol in normal saline. Overall synthesis time is 60 minutes EOB, and batch yields were 0.54-1.1 GBq (20-40 mCi), with radiochemical purity greater than 99% and specific activity exceeding 37 TBq/mmole (1,350 Ci/mmole).

In vitro cell uptake studies show that MDA-MB-468 cells yield five-fold higher specific uptake of [^{11}C]PK than MCF-7 cells, corresponding to the increased expression of PBR in MDA-MB-468 cells (*2*).

Biodistribution experiments demonstrate in MDA-MB-435 tumor-bearing mice a tumor to blood ratio of 4.4 (0.9901 vs. 0.2251 %ID/g; n=2) sixty minutes post-injection of [^{11}C]PK. A tumor to muscle ratio of 3.2 (0.9901 vs. 0.3112 %ID/g; n=2) was also seen at this time.

These studies suggest that further *in vivo* studies, including microPET imaging, of [^{11}C]PK in tumor-bearing mice are warranted.

This work was financially supported by the NIH Grant 1R24CA83060-1.

1. Beinlich, A., Strohmeier, R., Kaufmann, *et al.* (2000) *Biochemical Pharmacology* **60**, 397-402.
2. Hardwick, M., Fertikh, D., Culty, M., *et al.* (1999) *Cancer Research* **59**, 831-842.

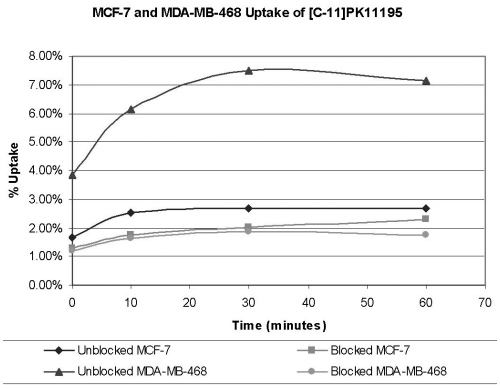

Keywords: [N-Methyl-^{11}C]PK 11195, Peripheral Benzodiazepine Receptor, Tumor

NOVEL SOMATOSTATIN PEPTIDOMIMETICS AS SOMATOSTATIN RECEPTOR SUBTYPE-2 SPECIFIC IMAGING AGENTS

G. Han,[1] H.F. Kung,[1,2] S.R. Choi,[1] S. Makonnen,[3] W. Lee.[3]
[1]Department of Radiology, University of Pennsylvania; [2]Department of Pharmacology, University of Pennsylvania; [3]Cancer Research Center, School of Medicine, University of Pennsylvania, Philadelphia, PA, United States.

Overexpression of somatostatin receptors (SSTRs) is strongly associated with various non-endocrine and endocrine tumors. Currently, there are only two FDA approved SSTR-targeting imaging agents, i.e, ^{111}In-DTPA-Octreodie (Octreoscan) and ^{99m}Tc-Depreotide (NeoTect). However, these imaging agents can't diagnose many tumors expressing SSTR2 accurately. In addition, both agents are peptide based and utilize *D*Trp^4-Lys as the binding motif. Due to the reactive and labile nature of the indole ring in *D*Trp^4, this moiety limits the flexibility in the development of new diagnostic imaging agents. Furthermore, both agents are designed only for Single Photon Emission Computed Tomography (SPECT). Thus, there is a need to develop improved imaging agents with the following advantages: 1) peptidomimmetics to demonstrate better biostability; 2) a better platform without *D*Trp to provide feasibility and versatility for chemical modification; 3) Positron Emission Tomography (PET) to achieve higher sensitivity and accuracy; 4) ^{18}F labeling to represent the preferred nuclide for routine PET imaging.

Fig. 1. SSTR peptidomimetic analogues.

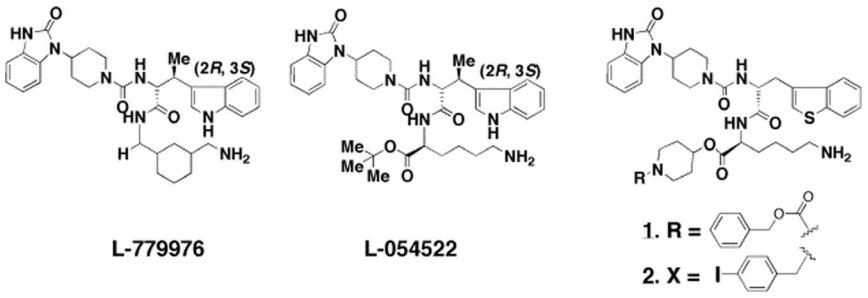

Hence, based on the highly selective SSTR2 peptidomimetics, **L-054522** and **L-779976** (**Fig. 1**), we can generate novel PET imaging agents for tumors overexpressing SSTR2. In our current design, we have substituted *D*Trp with less labile aromatic amino acids, *D*-benzo[*b*]thienylalanine (*D*Bta), which may provide an improved platform in designing SSTR peptidomimetic ligands. Consequently, we have a better opportunity to develop ^{18}F labeled imaging agents for PET imaging. Preliminary binding studies of these ligands (see examples in **Fig. 1**) using membrane preparations from K1735.m39 cells, which were transfected and cloned to overexpress human SSTR2 (hSSTR2) under a doxycyline-controlled expression, revealed that the K_i for **1 and 2** were 0.92 and 1.36 nM, respectively. The results suggest that these novel series ligands may represent a useful platform for developing SRIF peptidomimetics based imaging agents for various tumors overexpressing SSTR2.

Keywords: Somatostatin Receptors, Peptidomimetics, PET Imaging

EVALUATION OF ^{64}Cu- AND ^{86}Y-LABELED DOTA-(Pro^{1}, Tyr^{4})-BOMBESIN(1-14) A BOMBESIN ANALOGUE FOR TARGETING GRP RECEPTORS

G.B. Biddlecombe,[1] M. de Visser,[2] M. de Jong,[2] B.E. Rogers,[3] J.S. Lewis.[1]
[1]Mallinckrodt Institute of Radiology, Washington University School of Medicine, Saint Louis, MO, United States; [2]Department of Nuclear Medicine, Erasmus University Medical Center, Rotterdam, Netherlands; [3]Radiation Oncology, Washington University School of Medicine, Saint Louis, MO, United States.

Bombesin-derived peptides bind with a high affinity to gastrin releasing peptide (GRP) receptors. These receptors have been found in a variety of cancers including invasive breast and prostate tumors. (1, 2) The goal of this study was to investigate if radiolabeled DOTA-(Pro1, Tyr4)-Bombesin(1-14) would be a good candidate for the non-invasive detection of tumors using PET. It has been previously demonstrated that this peptide when labeled with In-111 (3) showed receptor-mediated uptake.

DOTA-(Pro1, Tyr4)-Bombesin(1-14) was labeled with either Cu-64 ($t_{1/2}$ = 12.7 h, $\beta+$ = 19.3%, Eavg = 278 keV) or Y-86 ($t_{1/2}$ = 14.7 h, $\beta+$ = 33%, Eavg = 664 keV) in ammonium acetate buffer at various concentrations, pH's and temperatures to optimize yields. Biodistribution of the radiolabeled peptides was investigated in mice bearing PC3 prostate tumors and rats bearing AR42J pancreatic tumors at 1, 4 and 24 hours post injection. Also, tumor uptake was confirmed using co-registered microPET/CT imaging (Concorde Microsystems Inc). An additional group of animals were co-administered 100 mg Tyr4-bombesin as a blockade and sacrificed at 1 h post injection.

DOTA-(Pro1, Tyr4)-Bombesin(1-14) was successfully labeled after 30 minutes with either Cu-64 or Y-86 at 80°C in 0.5 M NH4OAc (pH 5.5) in high radiochemical purity and specific activity. Biodistribution in PC3 tumor-bearing nude mice demonstrated a higher tumor uptake in mice injected with Y-86-DOTA-(Pro1, Tyr4)-Bombesin(1-14) than with the Cu-64-labeled peptide (1 h: Cu-64, 0.79 +/- 0.18 vs., Y-86, 2.65 +/- 0.12 %ID/g). Moreover, the Y-86 analog had significantly lower liver uptake (1 h: Cu-64, 1.33 +/- 0.30 vs., Y-86, 0.17 +/- 0.03 %ID/g). This can in part be attributed to the greater stability of the Y-DOTA chelate compared to Cu-64-DOTA. Receptor-mediated uptake of the radiolabeled peptides was confirmed by uptake in GRP receptor-rich tissues such as the pancreas (1 h: Cu-64, 4.39 +/- 1.09 vs., Y-86, 14.46 +/- 5.72 %ID/g) and by the significant reduction in uptake by co-injection of blockade in these tissues and the PC3 tumor. MicroPET/CT imaging in both the PC3 and AR42J tumor-bearing models confirmed specific uptake of the Cu-64 and Y-86 peptide in the receptor-rich tissues. As with the biodistribution studies, co-administration of blockade caused a significant reduction of uptake in these tissues, strongly suggesting a receptor-mediated uptake process. With the Y-86 images, it was easier to qualitatively delineate the tumors in the animals due to the lower uptake in clearance organs and low background activity.

We have successfully labeled DOTA-(Pro1, Tyr4)-Bombesin(1-14) with both Cu-64 and Y-86 for PET imaging of GRP receptors. The Y-86 analog demonstrated excellent image quality (microPET/CT) for the delineation of the two GRP receptor-rich tumor models and warrants further investigation. This work was supported by the National Cancer Institute (1 R24 CA86307).

1. Markwalder R, Reubi J.C. Gastrin-releasing peptide receptors in the human prostate: relation to neoplastic transformation. *Cancer Res*. 1999;59:1152-1159.
2. Gugger M, Reubi J.C. Gastrin releasing peptide receptors in non-neoplastic and neo-plastic human breast. *Am J Pathol*. 1999;155:2067-2076
3. Breeman et al., Preclinical Comparison of In-111-Labeled DTPA- or DOTA-Bombesin Analogs for Receptor Targeted Scintigraphy and Radionuclide Therapy. *J Nuc Med* 2002; 43:1660-1656

Keywords: GRP Receptors, microPET, Bombesin

A CANDIDATE HIGH AFFINITY β_1-ADRENOCEPTOR-SELECTIVE PET RADIOLIGAND: (*S*)-[*METHOXY*-^{11}C]-*N*-[2-[3-(2-CYANO-PHENOXY)-2-HYDROXY-PROPYLAMINO]-ETHYL]-*N′*-(4-METHOXY-PHENYL)-UREA (*S*)-[^{11}C]ICI-OMe)

K. Kopka,[1] M.P. Law,[1] S. Engelhardt,[2] B. Riemann,[1] V.W. Pike,[3] O. Schober,[1] M. Schaefers,[1] S. Wagner.[1]

[1]Department of Nuclear Medicine, Section Radiochemistry, University Hospital Muenster, Muenster, Germany; [2]Molecular Cardiobiology Group, DFG-Research Center for Experimental Biomedicine, Rudolf-Virchow-Center, University of Wuerzburg, Wuerzburg, Germany; [3]Molecular Imaging Branch, NIMH, NIH, Bethesda, MD, United States.

(*S*)-[^{11}C]CGP 12177 and (*S*)-[^{11}C]CGP 12388 represent the first non-subtype-selective β-adrenoceptor (β-AR) radioligands that have been clinically studied in man and that have succeeded for the *in vivo* visualization of cardiac and pulmonary β-AR density. Because of the predominant expression of the β_1-subtype in non-failing myocardium, the heart can be defined as a β_1-AR organ. Cardiac biopsies, however, suggest that, although myocardial β_1-AR density is reduced in patients with chronic heart failure, cardiac β_2-ARs may be decreased, unchanged or even increased. Therefore a PET technique for specifically quantifying β_1-AR densities in the human heart would be of great clinical interest.

We are developing PET radioligands based on the β_1-AR selective antagonist, ICI 89,406 (**1**) [1] and have shown that several derivatives possess high β-AR affinity as well as high β_1-AR selectivity, even when tested as racemates [3,4]. Here we describe the synthesis and ^{11}C-labeling of one promising candidate ([^{11}C]**2**; (*S*)-[^{11}C]ICI-OMe) for evaluation as a PET radioligand in rodents.

(*S*)-*N*-[2-[3-(2-Cyano-phenoxy)-2-hydroxy-propylamino]-ethyl]-*N′*-(4-methoxy-phenyl)-urea (**2**) (log D = -0.21 calculated by ACD/LogD Suite) and its desmethyl analog (**3**) were synthesized (overall yields, 26 and 14%, respectively) via multi-step convergent syntheses from the chiral epoxide (**4**) and the amines (**5**) (Figure 1).

Fig. 1 Synthesis and radiosynthesis of (*S*)-ICI-OMe (**2**) and its [*O-methyl*-^{11}C]-version ([^{11}C]**2**).

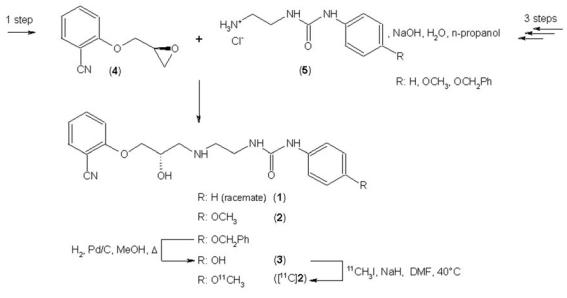

The β_1-AR binding affinity and selectivity of **2** were determined *in vitro* with mouse ventricular membranes and the non-selective β-AR ligand, [^{125}I]ICYP. The inhibition constants K_{I1} (β_1-ARs), K_{I2} (β_2-ARs) and β_1-selectivity (K_{I2}/K_{I1}) were found to be 0.067 nM, 83 nM and 1240, respectively.

[^{11}C]**2** was prepared by treating **3** (1 eq.) with NaH (14 eq.) and [^{11}C]iodomethane in DMF (200 µL) at 40°C for 5 min. After heating the reaction mixture to 50°C, water (200 µL) was added. This mixture was separated by HPLC (Nucleosil C18 pre-column; 100-10; 20 x 8 mm; Nucleosil 100-10 C18 column, 250 x 8 mm) eluted with 20 mM Na_2HPO_4-EtOH (4/1 v/v) at 4 mL/min. Collected [^{11}C]**2** (rt: 13.2 min) was obtained in 44% radiochemical yield (decay-corrected) in 97% radiochemical purity and with a specific radioactivity between 13 and 47 GBq/µmol (n = 14) within 41 min from the end of radionuclide production.

The high affinity and β_1-AR-selective candidate radioligand, (*S*)-[^{11}C]ICI-OMe ([^{11}C]**2**) is now being studied in wild-type mice and in transgenic mice which over express myocardial β_1-ARs (β_1TG4 mice) [4] using the high-resolution small animal PET scanner, quadHIDAC (Oxford Positron Systems).

References

1. ICI Ltd, London (UK), Patent CH 605666 1978; DE 2458908 1975; *Chem Abs.* 1976; **84**: 43599.
2. Kopka K. et al. *Bioorg Med Chem* 2003; **11**: 3513-3527.
3. Wagner S. et al. *Bioorg Med Chem* 2004; **12**: 4117-4132.
4. Engelhardt S. et al. *Proc Natl Acad Sci, USA* 1999; **96**: 7059-7064.

Keywords: beta1-Adrenoceptor Radioligand, ICI 89,406 Derivative, Carbon-11 Synthesis

NUCLEAR LOCALIZATION OF TWO ^{64}Cu-LABELED SOMATOSTATIN ANALOGS IN A CELL LINE STABLY TRANSFECTED WITH *SSTr2*

M. Eiblmaier,[1] B.E. Rogers,[2] C.J. Anderson.[1]
[1]Mallinckrodt Institute of Radiology, Washington University School of Medicine, St. Louis, MO, United States; [2]Department of Radiation Oncology, Washington University School of Medicine, St. Louis, MO, United States.

Introduction: ^{64}Cu-TETA-Y3-TATE and ^{64}Cu-CB-TE2A-Y3-TATE (Fig. 1) are two peptide analogs of somatostatin which showed SSTr2-specific uptake in AR42J rat pancreatic tumors in rats [1]. A427 human non-small cell lung carcinoma cells stably transfected with high levels of *SSTr2* were used to investigate nuclear uptake of ^{64}Cu from the chelator-Y3-TATE conjugates at different time points post-administration. Higher levels of ^{64}Cu in the nucleus might be correlated to enhanced tumor cell killing and would give information about the fate of these radiopharmaceuticals after internalization. The question to be addressed was whether the nuclear localization from ^{64}Cu-labeled somatostatin analogs stems from dissociation of ^{64}Cu from the chelator. We therefore examined two somatostatin analogs, where one analog was conjugated with a chelator known to form a very stable complex with ^{64}Cu (B).

Methods: Competitive receptor binding assays were performed to determine the IC_{50} of ^{64}Cu-TETA-Y3-TATE and ^{64}Cu-CB-TE2A-Y3-TATE on membranes of the A427 clone #7 (A427-7), which shows a high level of expression of *SSTr2*. Saturation receptor binding assays resulted in B_{max} and K_d values for this ligand-receptor interaction. Using these data, both radioligands were added to A427-7 cells and the distribution in cell medium, whole cells and nuclei was monitored over 24 h.

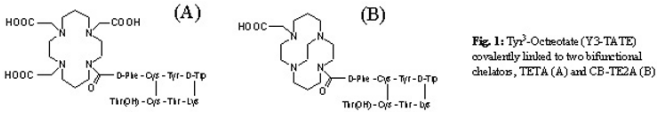

Fig. 1: Tyr^3-Octreotate (Y3-TATE) covalently linked to two bifunctional chelators, TETA (A) and CB-TE2A (B)

Results: On A427-7 cell membranes, ^{64}Cu-TETA-Y3-TATE was displaced with cold Cu-TETA-Y3-TATE with an IC_{50} value of 4.6 nM. In a saturation binding assay, the K_d of ^{64}Cu-TETA-Y3-TATE was 0.21 nM and the receptor concentration (B_{max}) of SSTr2 was 9,500 fmol/mg. The IC_{50} for ^{64}Cu-CB-TE2A-Y3-TATE displaced with the homologous cold compound was 3.7 nM. The K_d for ^{64}Cu-CB-TE2A-Y3-TATE was 0.69 nM and the B_{max} was found to be 32,750 fmol/mg; A substantially higher B_{max} for ^{64}Cu-(B) compared to ^{64}Cu-(A) has been observed previously with AR42J rat pancreatic tumor cells [1], and at this time, we have no explanation for the disparity of the SSTr2 receptor concentration found with two different ligands.

With AR42J cells and ^{64}Cu-TETA-octreotide, ~20% of internalized radioligand was found in the nucleus at 24 h [2]. A427-7 cells showed substantially increased uptake of both (A) and (B) compared to AR42J cells, with over 50% of added radioligand cell-associated within one hour. The activity found in the nuclear fraction increased from 1% of the cell-associated activity at 1 h to 14.5% at 24 h for (A), whereas for (B) no more than 1% of cell-associated radioligand was found in the nuclei at any time point. We hypothesize that ^{64}Cu dissociates from the chelator before entering the nucleus, and this finding supports earlier data suggesting higher *in vivo* stability for ^{64}Cu-CB-TE2A-Y3-TATE.

Acknowledgements: The authors would like to thank Susan Adams for technical assistance, Gary Weisman for supplying CB-TE2A and Samuel Achilefu, Kexian Liang, and Yunpeng Ye for peptide synthesis. The research was supported by NCI grants R01 CA064475 and R24 CA86307 (for ^{64}Cu production).

[1] Sprague J. E. et al., *Clinical Cancer research 10* (2004), 8674-8682.
[2] Wang M. et al, *Cancer research 63* (2003), 6864-6869.

Keywords: Copper-64, Somatostatin, Nuclear Uptake

TARGETED IMAGING OF PANCREAS β-CELL ACTIVITY WITH ^{99m}Tc-LABELED NATEGLINIDE

A. Azhdarinia, C. Oh, S. Kohanim, M. Chanda, D.-F. Yu, M. Ito, J.L. Bryant, E.E. Kim, D.J. Yang.
Experimental Diagnostic Imaging, University of Texas M.D. Anderson Cancer Center, Houston, TX, United States.

Purpose: In the pancreas, the beta cell comprised 60% of all cell types. Assessment of beta cell activity would provide early diagnosis of pancreas function and monitor drug treatment response on pancreatic beta cells. It also may provide patient selection of those who may respond to drugs. We hypothesize that if the binding of ^{99m}Tc-DTPA-nateglinide (DTPA-NGN2) to pancreatic beta receptor can be detected by gamma scintigraphy, this could, in turn, monitor the function of pancreas.

This study was aimed to develop a ^{99m}Tc-DTPA-NGN2 conjugate and to evaluate its feasibility to assess pancreas beta cell activity. **Methods:** Nateglinide (NGN) was converted to the ester form, followed by reaction with ethylenediamine and yielded amino analogue of NGN. DTPA dianhydride was conjugated to amino analogue of NGN, yielded 87% of two NGN conjugated. The synthetic scheme is shown in Fig 1. Biodistribution of ^{99m}Tc-DTPA-NGN2 was determined in F344 rats at 0.5-4 h. Planar imaging studies were conducted at 5-50 min post-injection of ^{99m}Tc-DTPA-NGN2 (300 μCi, i.v.). To demonstrate whether a receptor-mediated process occurred, rats were pretreated with NGN (4 mg/kg, ip) prior to receiving ^{99m}Tc-DTPA-NGN2. The images were acquired at 50 min post-administration. The effects on glucose levels after a single administration (i.p.) of two doses of DTPA-NGN2 were compared to the parent NGN (50,150 mg/kg). Blood glucose was measured immediately up to 6hrs. **Results:** Biodistribution of ^{99m}Tc-DTPA-NGN2 showed increased pancreas-to-muscle ratios whereas ^{99m}Tc-DTPA showed decreased ratios as a function of time. Planar images confirmed that the pancreas could be visualized with ^{99m}Tc-DTPA-NGN2 from 5 to 50 min. The image is shown in Fig 2. Rats pretreated with NGN could decrease pancreas uptake. The findings suggest that the pancreas uptake of ^{99m}Tc-DTPA-NGN2 was via a receptor-mediated process. DTPA-NGN2 showed better response in lowering glucose level compared to NGN. **Conclusion:** It is feasible to use ^{99m}Tc-DTPA-NGN2 to assess pancreas beta cell activity. This agent may be useful in evaluating patients with diabetes, pancreatitis and pancreatic tumors.

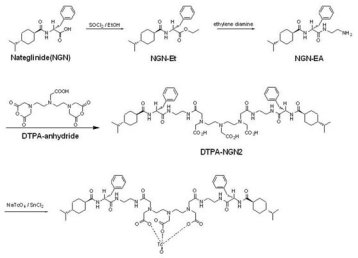

Fig 1. Synthesis of ^{99m}Tc-DTPA-NGN2

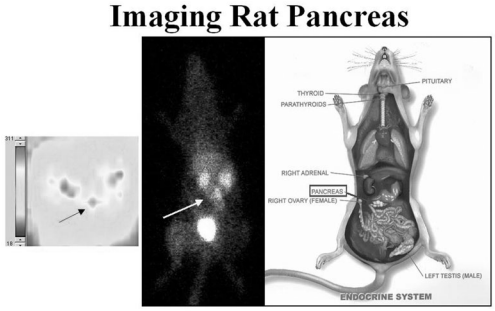

Fig 2. Mammary tumor-bearing rats were imaged with ^{99m}Tc-DTPA-NGN2 (300 μCi, i.v.). Selected planar images of ^{99m}Tc-DTPA-NGN2 are presented at 50 min post-injection. eZ scope also showed that pancreas could be imaged. Arrow designates pancreas.

Keywords: Beta Cell Imaging, Nateglinide, Technetium-99m

THE USE OF A BETA PLATE READER FOR RECEPTOR BINDING STUDIES USING ^{64}Cu, ^{177}Lu, AND ^{149}Pm

C.D. Sherman, W.P. Li, C.J. Anderson.
Mallinckrodt Institute of Radiology, Washington University School of Medicine, St. Louis, MO, United States.

Introduction: Receptor binding assays on cell membrane receptors are a frequent and important part of the process of developing new peptides for radiopharmaceuticals used in therapy and diagnosis. Radioactivity remaining on membrane-bound receptors at the end of an assay, sometimes up to 24 hours, may be too low to detect on a gamma counter. For isotopes that emit gamma and beta energy, a beta plate reader allows several advantages: higher counting efficiency, less sample processing and handling, and potential for high throughput screening of a small library of compounds.

Methods: ^{64}Cu was obtained from WU (St. Louis, MO), while ^{177}Lu and ^{149}Pm were obtained from MURR (Columbia, MO). To develop a method for using the beta plate reader (MicroBeta TriLux, Perkin Elmer Life Science), three factors were addressed: minimizing cross-talk (energy from one sample well being detected in an adjacent well), incubation period (determining the optimal time to capture maximum counts), and counting efficiency. To determine cross-talk, a 25 µL portion of known activity (gamma cpm) was added to one well of a filter plate (Millipore Multiscreen FB), dried in an incubator (37^{o} C), followed by addition of 25 µL of scintillation fluid (Wallac Optiphase SuperMix) to this well and four surrounding wells. Beta activity was measured in 1-2 h intervals for up to 20 h, and crosstalk was calculated in various energy windows as: (cpm adjacent)/(cpm central)*100. Optimal incubation period was determined by allowing plates of several levels of activity to run in 1-2 hour intervals up to 20 hours.

Results: For two of three radionuclides investigated, using a default energy window (allowing all beta energy to be measured) resulted in undesirable levels of crosstalk: 7-8% for ^{64}Cu, and 21% for ^{149}Pm. By redefining the energy windows to 220-700 and 281-741, respectively, crosstalk was reduced to 0.3% for ^{64}Cu, and <0.1% for ^{149}Pm. In the case of ^{177}Lu, crosstalk was low with the default energy window (0.06 – 0.2%, for a range of activity), making further modification unnecessary. Incubation periods varied by isotope: ^{64}Cu reached a plateau at 10 hours, ^{177}Lu at 15 hours, and ^{149}Pm exhibited a slow, steady increase to 18 hours. Counting efficiency varied greatly between isotopes (gamma abundance in parentheses): ^{64}Cu: 23% (5.5%); ^{177}Lu: 41% (10%); and ^{149}Pm: 65% (1.3%).

In addition, results of receptor binding data with both gamma and beta detectors validated the use of the beta plate reader. In a competitive binding assay with the somatostatin ligand, ^{64}Cu-DOTA-Y3-TATE in AR42J cell membranes yielded an EC50 value of 0.9177 nM for gamma counter counting vs. 0.9473 nM for beta plate reader counting; in a saturation binding assay of SST ligands, ^{177}Lu-DOTA-Y3-TATE yielded a Kd value of 1.008 nM for gamma counter counting, vs. 1.422 nM for beta plate reader counting; and, a competitive binding assay of ^{149}Pm-DOTA-Y3-TATE (vs. Sm-DOTA-Y3-TATE) on AR42J cell membranes yielded an EC50 value of 3.587 nM from beta plate reader. Due to the extremely low counting efficiency of ^{149}Pm on the gamma counter, we were not able to determine the EC50 using this method.

Conclusions: The data presented here show that the use of the beta plate reader in membrane-bound receptor-binding assays allows them to be done more efficiently and with greater sensitivity in the three radionuclides investigated. Comparing the beta-to-gamma ratios shows increased sensitivity by a factor of 4 for ^{64}Cu, 4 for ^{177}Lu, and 49 for ^{149}Pm.

Acknowledgements: This research was supported by NCI grants CA064475 and R24 CA086307 (for ^{64}Cu production).

Keywords: Beta Emitters, Receptor Binding Assay, Somatostatin

SYNTHESIS OF N-SUBSTITUTED 9-AZABICYCLO[3.3.1]NONAN-3α-YL PHENYLCARBAMATE ANALOGS AS SIGMA-2 RECEPTOR LIGANDS

W. Chu,[1] J. Xu,[1] K.T. Wheeler,[2] R.H. Mach.[1]
[1]Mallinckrodt Institute of Radiology, Washington University School of Medicine, St.Louis, MO, United States; [2]Department of Radiology, Wake Forest University School of Medicine, Winston-Salem, NC, United States.

Sigma receptors are a distinct class of proteins having a widespread distribution in the CNS and peripheral tissues. It is now widely accepted that there are two types of sigma receptors, σ_1 and σ_2. The σ_1 receptor has been cloned and has a molecular weight of ~25 kDa. The functions of these receptors are not yet clearly defined. An overexpression of σ_2 receptors has been reported in a variety of human and murine tumors.[1] The observation that the density of σ_2 receptors is greater in proliferating versus quiescent mouse mammary breast tumor cells grown in cell culture suggests that the σ_2 receptor is a potential receptor-based biomarker for imaging the proliferative status of solid tumors. In addition, it has been reported that σ_2 receptor ligands induce cell death in various breast tumor cell lines with features consistent with apoptosis.[2] Therefore, there is great interest in the developing a high affinity σ_2 receptor ligands to study the function of these receptors in proliferation and apoptosis, as well as for the development of PET and SPECT radiotracers for tumor imaging studies.

We previously reported that N-substituted 9-azabicyclo[3.3.1]nonan-3a-yl phenylcarbamate analogs have a modest affinity and selectivity for σ_2 vs σ_1 receptors.[3] The function of the current study was to expand the structure-activity relationship study on this class of compounds with the goal of identifying potential ^{11}C- and ^{18}F-labeled radiotracers for imaging the σ_2 receptor status of breast tumors. Therefore, a series of phenylcarbamate compounds (**1**) were synthesized and their affinity σ_1 and σ_2 receptors were measured. Compound **1h** (σ_1 = 1711 nM; σ_2 = 0.82 nM) and compound **1i** (σ_1 = 1437 nM, σ_2 = 0.08 nM) have the best affinity and selectivity σ_2 receptors. Radiolabeling of ^{18}F-**1h** and ^{11}C-**1i** are currently ongoing.

Acknowledgment. This research was supported by NIH grant CA102869 and the US Army Medical Research and Material Command under DAMD 17-01-1-0446.

References

Mach et al. Cancer Research **1997**; 57: 156-161.
Crawford et al. Cancer Research **2002**; 62: 313-322.
Mach et al. Medicinal Chemistry Research **2002**; 11: 380-398.

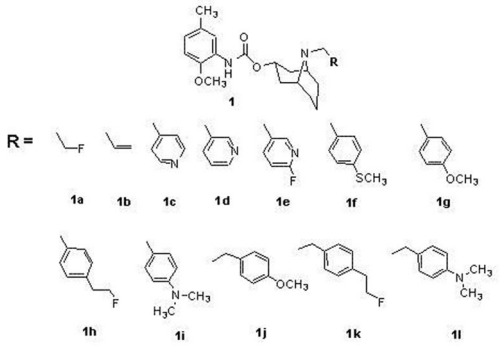

Keywords: sigma-2 Receptors Ligands, Breast Tumor, PET

POST MORTEM AUTORADIOGRAPHY OF THE HUMAN BRAIN NOREPINEPHRINE TRANSPORTER WITH (*S,S*)-[^{18}F]FMeNER-D$_2$

M. Schou,[1,2] C. Halldin,[1] V.W. Pike,[2] P.D. Mozley,[3] D. Dobson,[3] R.B. Innis,[2] L. Farde,[1] H. Hall.[1]
[1]Department of Clinical Neuroscience, Psychiatry Section, Karolinska Institutet, Karolinska Hospital, Stockholm; [2]Molecular Imaging Branch, National Institute of Mental Health, National Institutes of Health, Bethesda, MD, United States; [3]Eli Lilly Co., Indianapolis, IN, United States.

Introduction. *In vitro* autoradiographic studies of norepinephrine transporters (NETs) in the *post mortem* human brain have so far been performed using the radioligands, [^{3}H]desipramine, [^{3}H]mazindol and [^{3}H]nisoxetine [1-3]. Of these radioligands, [^{3}H]nisoxetine has been found to be the most suitable to examine NETs within the locus coeruleus (LC) and raphe nuclei but no other regions. The *O*-[^{18}F]fluoromethyl di-deuterated analog of (*S,S*)-[^{11}C]MeNER, namely (*S,S*)-[^{18}F]FMeNER-D$_2$ has high affinity (K_i = 3.1 nM) for NETs *in vitro* and has been found to bind selectively to NETs in the monkey brain *in vivo*. The aim of this study was to examine and characterise the potential of (*S,S*)-[^{18}F]FMeNER-D$_2$ as a radioligand for *in vitro* examination of NETs in the *post mortem* human brain.

Methods. (*S,S*)-[^{18}F]FMeNER-D$_2$ was prepared as previously described [4]. Sections from three human brains were obtained for this study from the National Institute of Forensic Medicine, Karolinska Institutet (Stockholm, Sweden). The sections were incubated with (*S,S*)-[^{18}F]FMeNER-D$_2$ (4 MBq, 148 GBq/μmol), washed (three times) and dried before being exposed to Kodak Biomax MR film overnight. Non-specific binding was estimated by simultaneous incubation with desipramine (10 mM). Competition studies were also performed with i) PE2I, a selective dopamine transporter (DAT) inhibitor ii) citalopram, a selective serotonin transporter (SERT) inhibitor, and iii) duloxetine, a dual NET and SERT inhibitor.

Results. A conspicuous accumulation of radioactivity was observed in the LC. Considerably lower radioactivity was seen in the cerebellum, cortex, thalamus or hypothalamus. The binding in these regions was abolished in cryosections incubated with desipramine, indicating specific accumulation of (*S,S*)-[^{18}F]FMeNER-D$_2$ at NET. Some labelling was also seen in the caudate nucleus and putamen, although this labelling was not abolished by the inclusion of desipramine in the incubate. The specific binding was reduced by over 95% after co-incubation with duloxetine, resulting in autoradiograms similar to those obtained in the presence of desipramine. The labelling of any brain region with (*S,S*)-[^{18}F]FMeNER-D$_2$ was unaffected by co-incubation with the DAT inhibitor, PE2I, or the SERT inhibitor, citalopram.

Discussion. (*S,S*)-[^{18}F]FMeNER-D$_2$ is a useful radioligand for imaging NETs within the LC of the *post mortem* human brain. However, the signal to noise ratio is significantly lower outside the LC, reflecting the lower densities of NETs. In addition to using (*S,S*)-[^{18}F]FMeNER-D$_2$ for LC, it seems crucial to develop a selective radioligand with markedly higher affinity for NET to enable *in vitro* visualization and quantification of NETs in regions external to LC.

References:

1. Ordway, G., et al. (1997) J Neurosci. 17:1710-1719.
2. Gross-Isseroff, R., et al. (1988) Brain Res 456:120-126.
3. Donnan, G., et al., et al. (1991) J Comp Neurol 304:419-434.
4. Schou, M., et al., (2004) Synapse 53:57-67.

Acknowledgement: This project was supported by Eli Lilly (USA).

Keywords: Norepinephrine Transporter, Autoradiography, Human Brain

THE NET RADIOLIGAND (*S,S*)-[^{11}C]MeNER PRODUCES A LIPOPHILIC LABELED METABOLITE MEASURED IN HUMAN PLASMA

M. Schou,[1,2] V.W. Pike,[2] B. Andree,[1] B. Gulyas,[1] E. Shchukin,[1] L. Farde,[1] C. Halldin.[1]
[1]Department of Clinical Neuroscience, Psychiatry Section, Karolinska Institutet, Karolinska Hospital, Stockholm, Sweden; [2]Molecular Imaging Branch, National Institute of Mental Health, National Institutes of Health, Bethesda, MD, United States.

Introduction. (*S,S*)-[^{11}C]MeNER (1) is a selective and potent NET inhibitor, that has recently been applied as a radioligand for quantification of NETs in the human brain *in vivo* (2). The aim of this study was to assess the extent and nature of the metabolism of (*S,S*)-[^{11}C]MeNER in human plasma and to examine possible differences in metabolism between monkeys and humans.

Biotransformations of (*S,S*)-[^{11}C]MeNER may be expected to be similar to those already known for reboxetine (the simple *O*-ethyl analog of (*S,S*)-[^{11}C]MeNER) (Scheme 1).

Scheme 1. Putative metabolism scheme based on the metabolism of reboxetine (3), which is an *O*-ethyl analog of MeNER.

Methods. Blood was sampled at four or five time-points after administration of (*S,S*)-[^{11}C]MeNER to human (n = 18) or cynomolgus monkey (n = 5), respectively, and centrifuged. Supernatant plasma was deproteinized with acetonitrile. Each acetonitrile-plasma mixture was measured in a well-counter and analyzed on a gradient reverse phase HPLC system with eluate monitored for radioactivity.

Results. The recovery of radioactive material from the HPLC column was 92 ± 7% (n = 7). The plasma radioactivity represented by unchanged (*S,S*)-[^{11}C]MeNER (Figure 1, fraction II, retention time (t_R) 5.7 min) in the human subjects decreased from 88 ± 5% at 4 min after injection to 82 ± 7% at 40 min (Figure 1). A more polar labeled metabolite eluted unretained from the HPLC column (fraction I) and increased from 3 ± 3% to 16 ± 7% of plasma radioactivity at 40 min.

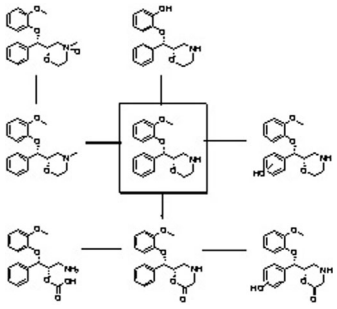

Figure 1. Time-course for the metabolism of (*S,S*)-[^{11}C]MeNER measured in human and monkey plasma.

The more lipophilic labeled metabolite, fraction III (t_R 7.5 min), decreased from 9 ± 5% at 4 min to 1 ± 2% at 40 min. The plasma radioactivity represented by (*S,S*)-[^{11}C]MeNER in monkeys decreased from 97 ± 2% at 4 min to 74 ± 7% at 45 min, with the polar fraction I as the major labeled metabolite. Fraction III was 3 ± 2% at 4 min and was not quantifiable at later time-points.

Discussion. A labeled lipophilic metabolite was observed and measured in monkey and human plasma after intravenous injection of (*S,S*)-[^{11}C]MeNER. Its rate of formation and clearance is species-dependent, with the highest level present in human plasma early after injection. The lipophilic labeled metabolite is cleared from human plasma before the data for estimating binding potential are obtained (AUC, 63-93 min (2)) and therefore is unlikely to confound PET measurements of NET made with (*S,S*)-[^{11}C]MeNER. Efforts are now being made to identify this metabolite.

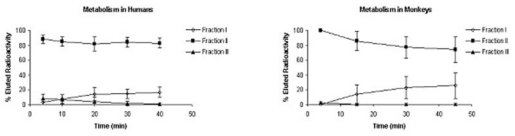

References:

1. Schou, M., et al. (2003) Nucl Med Biol, 30:707-714.
2. Andrée, B. et al. (2004) 51st Annual Meeting Scientific Abstracts of the Society of Nuclear Medicine. The Society of Nuclear Medicine, Philadelphia, pp 68-69, No. 193.
3. Dostert, P. et al. (1997) Eur Neuropsychopharmacol, Suppl 1:S23-35; discussion S71-3.

Keywords: Norepinephrine Transporter, MeNER, Metabolism

RADIONUCLIDE THERAPY USING ^{111}In-LABELED SOMATOSTATIN ANALOGS; SOMATOSTATIN RECEPTOR EXPRESSION IN A RAT TUMOR MODEL BEFORE AND AFTER THERAPY

M. De Jong, A. Capello, B. Bernard, W. Breeman, E. Krenning.
Nuclear Medicine, Erasmus MC, Rotterdam, Netherlands.

Peptide receptor scintigraphy with the radioactive somatostatin analog ^{111}In-DTPA-octreotide is a sensitive and specific technique to visualize the presence of somatostatin receptors on various tumors. ^{111}In not only emits gamma-rays, but also therapeutic Auger electrons with a very short tissue penetration (0.02-10 μm), therefore ^{111}In-DTPA-octreotide is also being used for clinical peptide receptor radionuclide therapy (PRRT).

In this study we investigated the therapeutic effects of ^{111}In-DTPA-octreotide in tumors of various sizes. After PRRT with ^{111}In-DTPA-octreotide, tumors can regrow because of the lack of crossfire. Possible receptor-negative tumor cells will not be irradiated and multiply. We therefore also investigated the somatostatin receptor status on tumors before and after PRRT.

Therapy with ^{111}In-DTPA-octeotide in small and larger tumors. We investigated the radiotherapeutic effects of different doses ^{111}In-DTPA-octreotide (111- 1110 MBq) in Lewis rats bearing small (< 1 cm^2) or larger (> 8 cm^2) rat pancreatic CA20948 tumors expressing somatostatin receptor subtype 2 (sst_2). Impressive radiotherapeutic effects of ^{111}In-labeled octreotide were found, estimated tumor radiation doses were 6.3 – 7.8 mGy/MBq (1 – 10 g tumor). Up to 50% complete responses were seen in the rats bearing small (< 1 cm^2) tumors after 1110 MBq ^{111}In-DTPA-octreotide, in the rats bearing the larger (> 8 cm^2) tumors the effects were much less pronounced and only partial responses were reached.

Low dose therapy to determine receptor expression. The somatostatin receptor densities were investigated in tumors isolated from the animals either when tumors were declining in size after low dose PRRT or later when tumors re-grew after initial size decline. Receptor density was determined using in vitro autoradiography on frozen microscopic tumor sections.

All tumors (including tumors from control, i.e. non-treated, animals) expressed high densities of sst_2. A significantly higher tumor sst_2 density ($p < 0.001$) was, however, found in tumors re-growing after an initial decline in size following PRRT.

Conclusions: Therapy with ^{111}In-labeled somatostatin analogs is feasible and should preferably start as early as possible after tumor development. One might also consider the use of radiolabeled somatostatin analogs in an adjuvant setting after surgery of somatostatin receptor-positive tumors, to eradicate occult metastases. PRRT led to a significant increase in somatostatin receptor density in tumors re-growing after initial size decline. This will lead to a higher uptake of radiolabeled peptides using repeated therapeutic administrations.

Keywords: Octreotide, Radionuclide Therapy, Indium-111

SPECT IMAGING OF ONCOGENE OVEREXPRESSION USING ^{99m}Tc-LABELED NEUROTENSION PEPTIDE 8-13 (NT)

K. Zhang,[1] Y. Zhang,[1] R. An,[1] Z. Gao,[1] G. Yan.[2]
[1]Department of Nuclear Medicnie, Union Hospital, Huazhong University of Science and Technology, Wuhan, Hubei, China; [2]College of Chemistry, Wuhan University, Wuhan, Hubei, China.

Objects To prepare neurotension peptides (NT) labeled with ^{99m}Tc for radiopharmaceutical application and evaluate the feasibility of SPECT imaging of oncogene NT receptors overexpressed in human colon cancer cells.

Methods NT analog, His-NT (8-13) was synthesized that histidine was attached at the N-terminus. The analogue was labeled with organometallic aquaion [^{99m}Tc$(H_2O)_3(CO)_3$] at pH 7. In vitro stability of ^{99m}Tc-NT was determined by challenging the compound with 100 times excess of DTPA, HSA and cysteine. The affinity, ^{99m}Tc-NT binding to the cell of carcinoma of colon, was studied in vitro. Biodistribution studies were performed at 4 and 12h respectively after ^{99m}Tc-NT was injected, and tissue distribution after receptor blocking was also performed at 4h in nude mice bearing colon carcinoma. Imaging with ^{99m}Tc-NT was performed at different time post-injection in nude mice bearing colon carcinoma, and imaging after receptor blocking was also performed at 4h post-injection.

Result The affinity constant that ^{99m}Tc-NT binds to the cells of colon carcinoma was obtained (K_d=0.91nmol/L). When ^{99m}Tc-NT was challenged with 100 times of DTPA, HSA, or cysteine, more than 97% radioactivity remained as ^{99m}Tc-NT. Biodistribution showed that the ratio of tumor to muscle was 2.85%±1.02%ID/g at 4h and 3.25%±1.46%ID/g at 12h postinjection respectively; ^{99m}Tc-NT was excreted chiefly from kidneys in vivo in nude mice bearing colon cancer. In receptor-blocking mice treated with unlabeled NT, the uptake of ^{99m}Tc-NT decreased in tumor and the ratio of tumor to muscle at 4h (1.21%±0.62%ID/g) is significantly lower than that (2.85%±1.02%ID/g) in receptor-unblocking mice treated without unlabeled NT. The ratio of tumor to contra lateral limb (2.68±0.44) at 4h postinjection obtained by technique of region of interest (ROI) was significantly higher than that (1.14±0.36) at 4h postinjection in receptor-blocking mice.

Conclusion The results suggest that the ^{99m}Tc-NT specifically binding to colon carcinoma cell and the significantly greater tumor uptake of ^{99m}Tc-NT, made ^{99}Tc^{m}-NT highly desirable for further studies in SPECT imaging of oncogene receptors overexpressed in colon cancer.

Keywords: Neurotension Peptide Receptor, Tumor, SPECT Imaging

SYNTHESIS AND EVALUATION OF NOVEL [^{123}I]-LABELLED BENZAMIDES FOR IMAGING MELANOMA

T. Pham, A. Katsifis, F. Mattner, X. Liu, P. Berghofer, I. Greguric, P. Ballantyne, J. Chapman, T. Jackson, V. Papazian, L. Berwick, V. Nguyen, B. Dikic, C. Loc'h.
Radiopharmaceuticals Research Institute, ANSTO, Sydney, NSW, Australia.

Introduction: Iodobenzamides have been proposed as potential imaging agents for melanoma. Consequently a large number of compounds based on these structures have been prepared and studied in B-16 animal tumour models with the prototypical ligands BZA and BZA2 also being studied in melanoma patients with encouraging results. Based on these lead structures, we have synthesised several new [^{123}I]labelled compounds with enhanced tumour uptake and retention. Here we report the synthesis, and *in vivo* evaluation of several lead [^{123}I]benzamides in B-16 and A375 melanoma tumours.

Methods: All non-radioactive benzamides and their radiolabelling precursors were prepared by standard synthetic methods. The radiolabelled derivatives were prepared by standard [^{123}I]iododestannylation or thaliation reactions in ethanol using chloramine-T as oxidant. Purification was achieved by C-18 semi-preparative HPLC, whilst radiochemical purity and specific activity (SA) were determined by analytical HPLC. All benzamides were also tested *in vitro* for σ-receptor binding affinity. Biodistributions of the lead ^{123}I-benzamides was undertaken in B16 and A375 mouse melanoma tumour models with analysis up to 48h p.i. *In vivo* imaging was performed on an X-SPECT scanner in both animal models following anaesthesia with isofluorane gas. Blocking studies with haloperidol were performed on selected compounds.

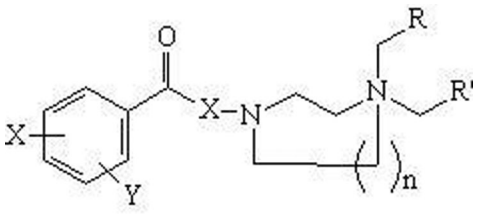

Results: [^{123}I]Radiolabelling was achieved in 73-85% radiochemical yield and >98% radiochemical purity. The *in vivo* biodistribution of the [^{123}I] tracers indicated high uptake in the B-16 melanotic tumour model 10-13% ID/g, but no-uptake in the A375 amelanotic tumoured mice. Tumour uptake was observed as early as 5 min peaking at 24h. Imaging studies over a 48 h time period in both mouse models paralleled that of the biodistribution study. Imaging indicated high uptake in tumour tissue in B-16 with rapid clearance from other organs.

Conclusion: A large number of [^{123}I]substituted iodo benzamides have been synthesised, radiolabelled with iodine-123 and their *in vivo* biodistribution and imaging undertaken. The high-uptake in B-16 melanotic tumours and virtually no uptake in the amelanotic A375 animals confirmed that the cellular uptake mechanism was due to melanin binding.

Keywords: Benzamides, SPECT, Melanoma

INTERACTION OF THE ANTITUMOUR METALLOCENE MOLYBDOCENE DICHLORIDE WITH BIOMOLECULES

K.S. Campbell,[1] C.T. Dillon,[2] M.M. Harding,[1] S.V. Smith.[3]
[1]School of Chemistry, The University of Sydney, Sydney, NSW, Australia; [2]Chemistry Department, University of Wollongong, Wollongong, NSW, Australia; [3]Materials and Engineering Science, ANSTO, Menai, NSW, Australia.

Interest in the bioorganometallic chemistry of metallocene dihalides has stemmed from the potent antitumour properties of titanocene dichloride (Cp_2TiCl_2; Cp=cyclopentadienyl) in clinical studies.[1,2] While *in vitro* studies have shown that molybdocene dichloride (Cp_2MoCl_2) has antitumour effects in Ehrlich ascites tumours,[1] currently there is insufficient biological data available to determine whether Cp_2MoCl_2 has potential for clinical development.[3,4] The present study explores the production and use of $Cp_2{}^{99}MoCl_2$ as a probe for studying the mechanism of antitumour action.

$Cp_2{}^{99}MoCl_2$ was prepared by neutron irradiation of the natural occurring Cp_2MoCl_2 in High Flux Australian Reactor (HIFAR) at ANSTO. The irradiated sample was characterised by UV spectroscopy and instant thin layer chromatography. The binding of $Cp_2{}^{99}MoCl_2$ to calf thymus DNA (ctDNA) and human serum albumin (HSA) were determined at varying concentrations at 37 °C. ctDNA and HSA were precipitated and supernatant counted in a gamma counter. Figure 1 shows the moles of Cp_2MoCl_2 bound to protein at various time intervals. Despite the much higher concentrations of DNA, there is significantly more binding of Cp_2MoCl_2 to HSA than to DNA. These results were compared with GFAAS analysis of subcellular fractions, as well as coordination studies. Collectively, they demonstrate that there is negligible interactions between Cp_2MoCl_2 and DNA. Cytotoxic effects of Cp_2MoCl_2 on V79 Chinese hamster lung cells are also consistent with Cp_2MoCl_2 targeting proteins *in vivo*, not DNA. The low binding of Cp_2MoCl_2 with ctDNA correlates well with recently reported ICP-AES results and NMR investigations.

In summary, these results demonstrate that the use of radiotracers has significant potential as a method to allow the analysis of whole cell fractions (nucleus, cytoplasm and subcellular fractions containing specific organelles), and hence provide important mechanistic information regarding Cp_2MoCl_2.

1. Kopf-Maier, P.; Kopf, H. *Drugs of the Future* **1986**, 11, 297.
2. Christodoulou, C. V.; Ferry, D. R.; Fyfe, *et al J. Clin. Oncol.* **1998**, *16*, 2761.
3. Harding, M. M.; Mokdsi, G. *Curr. Med. Chem.* **2000**, *7*, 1289.
4. Waern, J. B.; Harding, M. M. J. *Organomet. Chem.* **2004**, 689, 4655 and references cited therein.

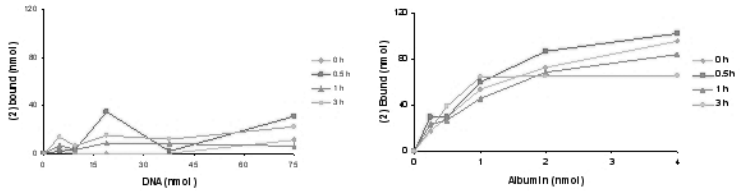

Figure 1. Cp_2MoCl_2 bound to ctDNA and HSA vs time.

Keywords: Molybdocene, Metallocene, In Vitro

CHARACTERIZATION OF *IN VIVO* RAT METABOLITES OF [*O-METHYL*-^{11}C]RWAY BY LC-MS

H.U. Shetty, S.S. Zoghbi, J.A. McCarron, J.-S. Liow, J. Hong, V.W. Pike.
MIB, NIMH, Bethesda, MD, United States.

Introduction. Detailed metabolic information is useful for designing new radioligands for molecular imaging. [*carbonyl*-^{11}C]WAY-100635 is effective for imaging brain 5-HT$_{1A}$ receptors *in vivo*, but suffers from rapid metabolism by amide hydrolysis (1). Therefore, we have explored [*O-methyl*-^{11}C]RWAY (**1**) as an alternative radioligand, since reversal of the direction of the amide bond may confer resistance to amide hydrolysis and make acceptable easy labeling at its *O*-methoxy group. **1** is a promising radioligand (2). Hence, we became interested in its *in vivo* stability. We found that the rat urine radiometabolite composition of **1** mirrors that of plasma. This fact opened an opportunity to identify the metabolites of RWAY (**2**), and hence of **1**, (Figure 1) without interference from protein or lipid. Herewith, we present LC-MS methodology for this purpose without resorting to *in vitro* enzymatic, cell cultures, or cell fractions to obtain partial information.

Experimental. One Sprague Dawley rat (300 g) was injected with **1** (1.0 mCi) and another with **2** (500 μg). The radioactive and non-radioactive animals were killed at 30 min and 2.4 h after injection, respectively. Urine and plasma samples were collected from both animals. The radioactive samples were analyzed by RP-radio-HPLC. The LC-MS analysis of urinary metabolites (non-radioactive) involved HPLC separation on a C18 column, electrospray ionization and MS and MS-MS detections using ThermoFinnigan's LCQ Deca instrument.

Results and Discussion. In rat administered with **1**, the urine and plasma radiometabolite profiles were found to be comparable. LC-MS analysis of the urine sample (from the non-radioactive experiment) generated mass spectral data that account for several of the metabolites predicted for **2**. The metabolic pathways, aromatic hydroxylation, aliphatic hydroxylation and *N*-dealkylation (Figure 1) are operative in the genesis of the metabolites so identified. In addition to the primary metabolites formed by these routes, the mass spectral data indicated the presence of significant amounts of dihydroxy metabolites in rat urine. The MS-MS data for each metabolite showed specific fragment ions assignable to the structure and/or the expected mass shift from fragment ions of **2**. The *m/z* values for fragment ions allowed differentiation of hydroxy metabolites generated by aromatic and aliphatic hydroxylation pathways. In contrast to the presence of these expected metabolites, there appear to be no metabolites generated by hydrolysis of the amide bond in **1 or 2**.

Conclusions. Plasma metabolites are generally eliminated by renal excretion and thus radiometabolite profiling and characterization of the non-radioactive metabolites of **2** was possible using urine samples. No sample preparation was involved as this body fluid is mostly devoid of protein and lipid molecules. The metabolite screening by MS indicated that the amide bond in **1 or 2** is metabolically stable, unlike that in its structural analog, WAY-100635. Identification of these urinary metabolites may help to characterize the radiometabolites of **1** that possibly enter and accumulate in brain. Finally, in addition to their identification, radioligands and their metabolites can be quantified using the highly sensitive LC-MS-MS technique (3).

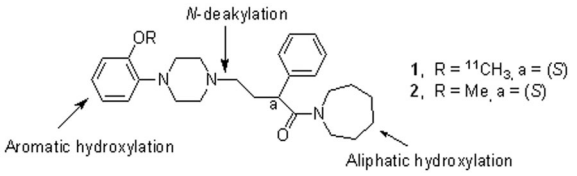

Figure 1. Structures of **1** and **2.**

References:
1. Osman S et al. *Nucl Med Biol* 1998; 25: 215–223.
2. McCarron JA et al. *NeuoroImage* 2004; 22 (Suppl. 2): T34-T35.
3. Shetty HU. et al. *J Label Compd Radiopharm* (In Press).

Keywords: Metabolites, LC-MS, Radioligand

[6- OR 7-METHOXY-^{11}C]PD153035: DOES THE LABELING POSITION INFLUENCE THE LABELED METABOLITES GENERATED?

J.-O. Thorell,[1] A. Fredriksson,[1] E. Samen,[1] S. Stone-Elander.[1,2]
[1]Research Dept, Karolinska Pharmacy, Stockholm, Sweden; [2]Clinical Neurosciences, Karolinska Institute & Hospital, Stockholm, Sweden.

PD 153035 (4-(3-bromoanilino)-6,7-dimethoxyquinazoline, 1) is a potent inhibitor selective for the epidermal growth factor receptor-tyrosine kinase, EGFR-TK, (Ki = 5.2 pM, IC50 = 29 pM) (1). It has previously been labeled with [^{11}C]CH_3I in the 6-methoxy position, 2b, (2) and with [^{11}C]CH_3OTf in the 7-methoxy position, 3b, (3). The resulting radiotracer was shown to have promising characteristics in vitro (3) and in vivo in rats (4). Since the corresponding *O*-demethylated compounds, 2a and 3a, have been detected after administration of large doses of PD153035 in mice (5) and both have affinity for the EGFR, a possible difference in the rate of the production of the labeled metabolites, 2c and 3c, could be of importance for the choice of labeling position for in vivo imaging applications.

Therefore, both *O*-desmethyl precursors, 2a and 3a, were synthesized in 7 steps starting from the corresponding monomethoxy-monohydroxy-benzoic esters and were labeled by the method in (2). The in vitro metabolism of 2b and 3b in rat liver microsomes was examined using the method described in (6). Samples were taken at 5, 15, 30, 45 and 60 min. Metabolite analysis was performed by HPLC (μ-Bondapak C18 (300x7.8 mm); CH_3CN:H_2O:TFA=30:70:0.1; 6 mL/min) requiring 20 min per sample. Eluents were collected in 30 sec fractions and the radioactivity was measured in a well counter.

Labeled 2c and 3c arising from *O*-demethylation were observed in only very small amounts (<1%) during the 1 hr incubation. Nor was $^{11}CH_3OH$ formed in any significant amounts. Instead, with both 2b and 3b, almost exclusively one major metabolite was observed (eluted with the same retention time and immediately before the reference 6,7-di-desmethyl compound 4). Since the pattern of metabolism was so similar for 2b and 3b, it appears that the choice of which methoxy to label will most likely not influence the in vivo results during a 1 hr scan. This in vitro assay was instrumental in screening for metabolic patterns prior to corroboration of behavior in vivo, most probably with fewer samples of lower radioactivity.

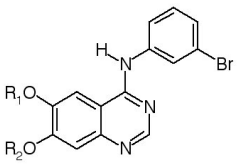

	R_1	R_2	T_{ret} (min)
1	CH_3	CH_3	12.8 -14.2
2a	H	CH_3	8.2 - 9
2b	$^{11}CH_3$	CH_3	*as 1*
2c	$^{11}CH_3$	H	*as 3a*
3a	CH_3	H	10 -10.9
3b	CH_3	$^{11}CH_3$	*as 1*
3c	H	$^{11}CH_3$	*as 2a*
4	H	H	7 - 8

Financial support by Cancerfonden (4722-B03-02XBB) is gratefully acknowledged.

1. Fry DW, Kraker AJ, McMichael A, Ambroso LA, Nelson JM, Leopold WR, Connors RW, Bridges AJ. *Science* 1994; **265**: 1093-1095.
2. Johnström P, Fredriksson A, Thorell J-O, Stone-Elander S. *J Label Compd Radiopharm* 1998; **41**: 623-629.
3. Mulholland GK, Zheng Q-H, Winkle WL, Carlson KA. *J Nucl Med* 1997; **38** P141.
4. Fredriksson A, Johnström P, Thorell J-O, von Heijne G, Hassan M, Eksborg S, Kogner P, Borgström P, Ingvar M, Stone-Elander S. *Life Sci* 1999; **65**: 165-174.
5. Kunkel MW, Hook KI, Howard CT, Przybranowski S, Roberts BJ, Elliott WL, Leopold WR. *Invest New Drugs* 1996; **13**: 295-302.
6. Lee S-Y, Choe YS, Kim DH, Park B-N, Kim SE, Choi Y, Lee K-H, Lee J, Kim B-T. *Nucl Med Biol* 2001; **28**: 391-395.

Keywords: PD153035, Epidermal Growth Factor Receptor- Tyrosine Kinase, In Vitro Metabolism

A NOVEL F-18 LABELED σ^2 RECEPTOR LIGAND FOR IMAGING BREAST CANCER

Z. Tu,[1] J. Xu,[1] L.A. Jones,[1] S. Li,[1] K.T. Wheeler,[2] M.J. Welch,[1] R.H. Mach.[1]
[1]Radiology Department, Radiological Science, Washington University School of Medicine, St. Louis, MO, United States; [2]Radiology Department, Wake Forest University School of Medicine, Winston-Salem, NC, United States.

Sigma (σ) receptors are a distinct class of receptors that are expressed in many normal tissues, including liver, kidneys, endocrine glands and the central nervous system. It has been well established that there are two types of σ receptors, σ_1 and σ_2. Several studies have reported an overexpression of σ_2 receptors in both human and murine tumors. Additional studies have shown the expression of σ_2 to be a reliable biomarker for the proliferative status of solid tumors.[1] Therefore, radioligands having a high affinity and high selectivity for σ_2 vs. σ_1 receptors should be good tracers for the non-invasive assessment of the proliferative status of solid tumors using PET or SPECT.

We have previously reported the result of a series of ^{11}C-labeled conformationally-flexible benzamide compounds having a high affinity and outstanding selectivity for σ_2 receptors.[2] One compound, N-(4-(3,4-dihydro-6,7-dimethoxyisoquinolin-2(1H)-yl)butyl)-2-[^{11}C]-methoxy-5-methylbenzamide, has shown promise as a PET radiotracer for imaging breast tumors. In the present study, we report the synthesis, in vitro binding, and radiolabeling of a novel ^{18}F-labeled σ_2 receptor ligand, compound **A** (Figure) which has a high affinity for σ_2 receptors (Ki = 0.26 ± 0.07 nM) vs. σ_1 receptors (Ki = 2150 ± 412 nM). The presence of an ortho fluoroethoxyl group in compound **A** indicates that an ^{18}F-labeled radiotracer could be prepared. This was accomplished by microwave irradiation of the corresponding methanesulfonate ester precursor with [^{18}F]/F$^-$ to give **[^{18}F]A** in an overall yield of 25% and a specific activity of 2000 Ci/mmol.

Biodistribution studies were conducted in mature BALB/C mice that were implanted with EMT-6 mammary tumors. The mice were implanted in the scapular region 7 days prior to the study. Animals were injected with the ^{18}F-labeled radiotracer and sacrificed at 5, 30, 60, and 120 min post-i.v. injection of the radiotracer. The %ID/g uptake values in tumor were: 5.02 ± 0.55, 4.00 ± 0.24, 2.99 ± 0.17, 1.83 ± 0.28, respectively. The tumor:normal tissue ratios at 1 hr and 2 hr post-i.v. injection of the **[^{18}F]A** radiotracer are shown in the Table. MicroPET imaging studies also revealed a clear visualization of the tumor at 2 hr post-i.v. injection of the radiotracer. The results of this initial study indicate that **[^{18}F]A** is a potential radiotracer for imaging the σ_2 receptor status of breast tumors in vivo with PET.

Figure

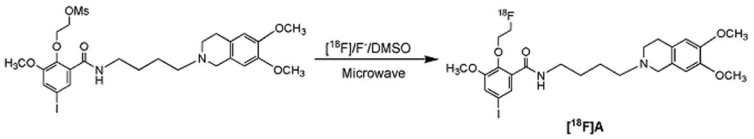

Table. Tumor:Normal Tissue Ratios of **[^{18}F]A**.

	1.0 hr	2.0 hr
Tumor : blood	3.40 ± 0.35	4.91 ± 0.68
Tumor : lung	1.42 ± 0.17	2.46 ± 0.39
Tumor : muscle	5.13 ± 1.62	7.17 ± 3.63
Tumor : fat	4.84 ± 1.17	8.38 ± 1.90

Acknowledgment. The authors would like to thank Dave Ficke, Pat Margenau and Bill Margenau for their excellent technical assistance. This research was supported by NIH grant CA102869 and the US Army Medical Research and Material Command under DAMD 17-01-1-0446.

References

Mach et al., Cancer Research **1997**; 57: 156-161.
Tu et al., J. Nucl. Med. **2004**; 45 (Supplement): 168.

Keywords: sigma Receptor, Tumor Proliferation, Carbon-11 Labeling

PHARMACOKINETICS AND BIODISTRIBUTION OF RADIOLABELED CHOLINE IN HUMAN SUBJECTS: COMPARISON OF [^{11}C]CHOLINE AND [^{18}F]FLUOROCHOLINE

S. Vallabhajosula, L. Kostakoglu, P.J. Kothari, K.A. Hamacher, S.J. Goldsmith.
Department of Radiology, Citigroup Biomedical Imaging Center, Weill Medical College of Cornell University, New York, NY, United States.

All cells utilize choline as a precursor for the biosynthesis of phospholipids, which are essential components of membranes. Carcinogenesis is characterized by enhanced cell proliferation. It has been suggested that malignant transformation of cells is associated with the induction of choline kinase activity resulting in increased levels of phosphorylcholine. In 1997, Hara, et al (1) developed [^{11}C]Choline (CH) to image brain, lung and prostate cancer using PET. One of the major problems of CH is the metabolism in blood. Within 30 min, most of the CH in blood is converted to a major metabolite [^{11}C]betaine. DeGrado et al in 2001 developed [^{18}F]Fluorocholine (FCH) and showed that fluorination of choline makes the molecule less susceptible for oxidation. In order to determine, biodistribution and dosimetry, DeGrado et al (2) performed PET imaging study in human subjects starting at 10-20 min after injection (only one time point) and used transmission images for attenuation correction. In order to understand the kinetics of distribution and optimize the radiation dosimetry, we designed a protocol to compare the pharmacokinetics of both CH and FCH in the same subject based on serial imaging studies.

FCH was synthesized using a modified FDG coincidence synthesis module. ^{18}F fluoride was reacted with dibromomethane to generate fluorobromomethane gas which reacted with N,N-dimethylaminoethanol (precursor) previously loaded on a C18 Sep-pak cartridge to produce FCH. The product was washed and purified using CM cartridge. CH was synthesized by reacting [^{11}C]CH_3I with the same precursor as above. Sterile filtered FCH or CH was collected in 3 mL saline. Quality control studies were performed using both TLC and HPLC. Each subject was injected with 148 MBq of FCH and 370 MBq of CH The PET imaging studies with both these tracers were performed within 10 days. Following administration of the dose, 3 PET imaging studies (6 frames, 3-4 min/frame) were performed starting at 5, 30 and 50 min. In order to reduce the radiation exposure to the subject, CT scans were acquired in a high speed with low current mode (Hs mode, pitch 6; Tube current, 10mA; tube rotation, 0.5 s).

To date 3 subjects with prostate cancer have had both CH and FCH studies. With both tracers, the clearance of radioactivity from circulation was very rapid; almost 70-80% activity cleared from Blood within 20 minutes. With both tracers liver has the highest uptake; 19-22% at 25 min followed by kidneys (7-9%) and spleen (4-5%). During the first hour, the liver activity with F-18 is relatively constant while there is a slight increase with C-11. The activity in the kidney and spleen gradually declined. The Figure below shows FCH and CH images obtained in the same subject at 30 min post injection. Urinary activity was seen only with FCH and the maximum activity in the bladder was <4% by 1 hour. The biodistribution data confirms similar biological handling of the two tracers except for metabolism of CH in blood. The data will be used to estimate radiation dosimetry.

1. Hara T, et al. PET imaging of brain tumor with [methyl-^{11}C] choline. J Nucl Med 1997; 38:842.
2. DeGrado TR, et al. Pharmacokinetics and Radiation Dosimetry of 18F-Fluorocholine. J Nucl Med 2002; 43:92.

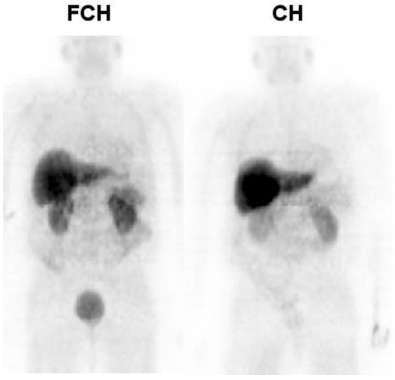

Keywords: Radiolabeled Choline, Proliferation, PET

EFFICIENT RADIOSYNTHESIS OF 5-[^{131}I]IODO-2′-FLUORO-DEOXYURIDINES AND BIODISTRIBUTION IN SCID MICE BEARING LYMPHOMA

K. Wczasek, A.T.J. Vogg, G.J. Cudek, B. Neumaier, S.N. Reske.
Nuklearmedizin, Universitatsklinikum Ulm, Ulm, Germany.

Aim

2´-Fluor stabilized nucleosides labelled with ^{131}I promise to be incorporated into DNA and therefore are candidates for endo radiotherapy (ERT). Two stereoisomers were synthesized by oxidative destannylation using Chloramine T: 5-Iodo-(1´-(2´-deoxy-2´-fluoro-β-D-arabinofuranosyl)uracil ([^{18}F]FIAU) and the ribo derivative ([^{18}F]FIUdR).

Methods

For the radiosynthesis 100 µL 5-trimethyl-stannyl precursor (ABX, 0.125 to 2 mg/mL in MeOH), 10 µL glacial acid, 1 to 500 MBq Na^{131}I (Amersham International), and 50 µL Chloramine T (0.05 to 1 mg/mL in H2O/MeOH (50/50, v/v)) were added to a sealed 2 mL ReactiVial (Alltech). The reactions were conducted at room temperature (21°C). For kinetic investigations 5 µL aliquots were taken, quenched with 50 µL 0.1 M thiosulfate solution (0.1 M) and analyzed by HPLC.

Analytical HPLC was performed using gradient RP chromatography. Conditions: flow 1 mL/min; eluents: H20 (A) and MeOH (B); conditions: 30 - 100 % (B) from 0 - 10 minutes, 100 % (B) (10 - 15 minutes), 100 - 30 % (B) (15 – 17 minutes); re-equilibration to minute 20; column: LiChrospher 100 RP EC-5 250*4; retention times [min]: 2.19 ([^{131}I]iodide), 3.41 ([^{131}I]by-product-1), 4.06 ([^{131}I]FIUdR), 4.44 ([^{131}I]FIAU), 5.97 ([^{131}I]by-product-2).

Preparative purification of both compounds was performed using similar conditions as in analytical HPLC, however starting the gradient differently: 15 - 100 % (B) within 0 - 15 minutes. The product fractions were collected, analyzed, evaporated and re-dissolved in isotonic NaCl solution. After final sterile filtration, the radiopharmaceuticals were ready for in vivo application.

Biodistribution studies were performed using SCID mice (23 gram) bearing human solid lymphoma induced by subcutaneous injection of 1E+6 cells of DoHH2 cells in the shoulder area 3 weeks before the biodistribution study. Tumor weight was 0.5 t o 0.8 gram. The radiopharmaceutical (100 µL) was injected via vein tail without anesthesia.

Results

The labelling kinetics of [^{131}I]FIUdR and [^{131}I]FIAU were examined in a time range 2 to 30 minutes at room temperature. After two minutes radiochemical yield (RCY) was 98.8 % and 99.5 after five minutes for both substances. Further investigations were made with [^{131}I]FIUdR. The optimal pH was found to be pH 2 (lowest amount of by-product-1). With increasing pH, by-product-1 increases (17.8 % at pH 8). Variation of Chloramine-T concentrations between 0.1 and 2 mg/mL showed no significant RCY change, but it dropped to 1 % at 0.05 mg/mL. Within the precursor concentration range of 0.125 to 2 mg/mL RCY´s were constant. Studies of the chemical stability of [^{131}I]FIUdR in cell incubation medium (RPMI1640, Gibco; FCS, Biochrom) at 37°C gave 1.6 % and 10.8 % free [^{131}I]iodide after 505 and 1410 minutes of incubation, respectively.

Biodistribution of [^{131}I]FIAU, the iodine analogue to [^{76}Br]BFU [1], after 60 minutes of incubation time showed only low tumor uptake of 1.5 % ID/g. Elevated concentrations were seen in kidneys (6 %) and stomach (5 % ID/g), indicating fast excretion and [^{131}I]iodide release, respectively. This findings were compared to that of the stereoisomer.

[1] Lu L., Samuelson L., Bergström M., Sato K., Fasth K.-J., Langström B., J. Nucl. Med. 43, 1688 (2002).

Keywords: Nucleosides, Endo Radiotherapy, Biodistribution

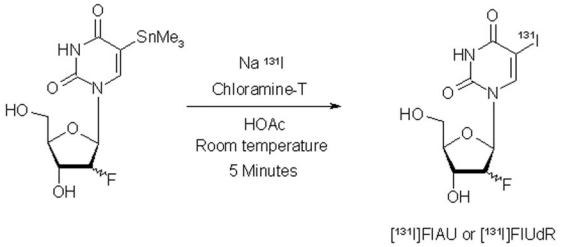

PRECLINICAL STUDIES OF 3′-DEOXY-3′-[^{18}F]FLUOROTHYMIDINE

S.J. Oh,[1] D.Y. Chi,[2] K.C. Im,[1] S.H. Kang,[1] J.S. Ryu,[1] S.Y. Kim,[1] S.J. Lim,[1] D.H. Moon.[1]
[1]Department of Nuclear Medicine, Asan Medical Center, College of Medicine Ulsan University, Seoul, Korea; [2]Department of Chemistry, Inha University, Incheon, Korea.

Purpose: [^{18}F]FLT is a new tumor cell proliferation imaging agent. We evaluated the cold FLT toxicity and ADME (Absorption, Distribution, Metabolism and Excretion) of [^{18}F]FLT in animals. **Methods**: (5′-*O*-Triphenylmethyl-3′-deoxy-3′-*O*-(4-nitrobenzenesulfonyl)-β-D-threopentafuranosyl) thymine as a precursor and cold authentic FLT supplied from FutureChem (Seoul, Korea). We used GE TracerLab MX module for the production of [^{18}F]FLT with automatic process. Toxicity studies were performed according to Korean GLP regulation with rats and beagle dogs. For rat studies, we injected 0-1,000 μg/kg of cold FLT for male and female rats (n = 5 for each group). For dog studies, we injected 333 μg/kg of cold FLT as 10,000 times of higher dose for human studies. After administration, we checked vital sign and death rate for two weeks. To find metabolites of [^{18}F]FLT, we injected 10 mg/kg of cold FLT to mouse and collected urine samples. Chemical structures of metabolites were droven by mass spectroscopy. In ADME studies, normal and tumor bearing mouse were used. For AD studies, 0.1 mCi/0.1 mL of [^{18}F]FLT were injected to mice and rats. For ME studies, 1 mCi/0.2 mL of [^{18}F]FLT were used. At 1, 15, 30, 60, 120, and 180 min after injection, animals were sacrificed and %ID/g of tissue samples were obtained. Liver, blood, urine and tumor metabolites samples were also analyzed with radioTLC (n = 3 for each group). For excretion studies, urine samples were collected until 6 h after injection. Three male normal beagle dogs (weight; 5.1 ± 0.3 kg) used for evaluation of pharmacokinetic parameters of [^{18}F]FLT by using dynamic PET images and anatomical information from PET/CT images. After transmission scan, dynamic PET images were acquired for 1 h using SIEMENS ECAT HR+ scanner after i.v. injection of [^{18}F]FLT 37 MBq/kg. Serial arterial blood sampling after injection of [^{18}F]FLT was done for obtaining input function. The PET image field of view included brain to lower abdomen. Then, dogs were transferred to PET/CT scanner on flat table without position change and whole body PET/CT images were acquired. Using anatomical information from PET/CT, the regions of interest (ROI) of heart, lung, liver, brain, bone marrow and small intestines were defined on dynamic PET images. From the time activity curve of each organ, C_{max}, T_{max}, area under curve (AUC) and clearance were obtained. **Results**: There were no death and no vital sign changes of rats or dogs after injection cold FLT. Urine samples with cold FLT showed two metabolites and they were unknown metabolite **1** (MW:257), FLT-monophosphate (MW:323), and FLT (MW:243). In AD studies, kidney showed the highest uptake for normal and tumor bearing mouse. Tumors showed higher uptake than other organs in tumor bearing mouse (1.29 ± 0.07 %ID/g for mice SCC 7 tumor at 1 h). We also found same three metabolites from obtained tissue, urine and blood with [^{18}F]FLT. Urine excretion ratios were 55.3 ± 9.1 and 72.8 ± 9.0% at 1 and 3 h for mice, respectively. T_{max} of [^{18}F]FLT in beagle dog blood was 0.08 min and bone marrow and small intestine showed high AUC value (2.12 ± 0.07 and 3.91 ± 0.82, respectively). But brain, lung and heart showed fast clearance (535.67 ± 159.25, 207.70 ± 24.28 and 131.34 ± 28.52 cc/min). We also found three metabolites from blood collection and found similar urine excretion ratio (81.6 ± 2.30% from injected dose). **Conclusion**: Preclinical studies showed [^{18}F]FLT was safe. ADME studies with mouse and beagle dogs showed high tumor uptake, rapid urine excretion and three metabolites were found.

Keywords: Fluorothymidine, Preclical Studies, Positron Emission Tomography

THE CASPASE INHIBITOR (*S*)-[*1-METHYL*-^{11}C]-1-(METHYL)-5-[1-(2-PHENOXYMETHYLPYRROLIDINYL)SULFONYL]ISATIN: A PUTATIVE NONPEPTIDYL CASPASE BINDING RADIOLIGAND

A. Faust,[1,3] S. Wagner,[1] P. Keul,[1,3] O. Schober,[1] B. Levkau,[2] M. Schaefers,[1,3] K. Kopka.[1,3]
[1]Department of Nuclear Medicine, Section Radiochemistry, University Hospital Muenster, Muenster, Germany; [2]Institute of Pathophysiology, Center of Internal Medicine, University Hospital Essen, Essen, Germany; [3]Interdisciplinary Center of Clinical Research (IZKF), University Hospital Muenster, Muenster, Germany.

Caspases (cysteinyl aspartate-specific proteases) belong to the enzyme class that represents the common final path of apoptosis. Thus, caspases are a suitable *in vivo* target for non-invasive molecular imaging of apoptotic tissues *in vivo*.

Radiolabeled Annexin V derivatives [1] were introduced as apoptosis detecting radiotracers that preferably bind to negatively charged phospholipids (i.e. phosphatidylserine) that externalize to the outer cellular membrane during apoptosis. In contrast 5-pyrrolidinylsulfonyl isatins represent a rare class of potent nonpeptidyl caspase inhibitors which bind selectively to the downstream effector caspases 3 and 7 [2]. Radiolabeled 5-pyrrolidinylsulfonyl isatins should result in Caspase binding Radioligands (CbRs) that form intracellular enzyme-inhibitor complexes by binding of the CbR to the activated caspase. The aim is to develop an exclusive imaging agent with high clinical impact to differentiate between balanced (physiological) and unbalanced culminated (pathological) apoptosis using PET.

Fig. 1 Synthesis route for the preparation of lead compound **1** and its ^{11}C-labeled CbR-version [^{11}C]**1**.

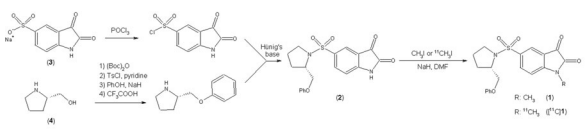

Non-radioactive **1** (logP = 2.27) that has been shown to possess cardioprotective potential in isolated rabbit hearts after ischemic injury [3] was chosen as lead structure. The radiochemical resynthesis of this therapeutic agent yielded [*1-methyl*-^{11}C]-CbR ([^{11}C]**1**), a putative marker of apoptotic tissues (Figure 1). The preparations of **1** and its desmethyl precursor (**2**) were achieved (overall yield, 18% and 33%, respectively) via multi-step convergent syntheses from 5-isatinsulfonic acid (**3**) and L-prolinol (**4**) [4] (Figure 1).

Inhibition of recombinant human caspase 3 by **1** was assessed using a standard fluorometric assay [5] (Inhibition constant $K_{i(app)}$ = 124 nM).

[^{11}C]**1** was prepared by treating **2** (1 eq.) with NaH (2 eq.) and [^{11}C]iodomethane in DMF (200 µL) at 80°C for 5 min. After cooling the reaction mixture to 50°C, water (200 µL) was added. This mixture was separated by HPLC (Nucleosil C18 pre-column 100-10, 20 x 8 mm; Nucleosil 100-7 C18 column, 250 x 16 mm) eluted with H_2O/CH_3CN (65/35 v/v) at 4 ml/min. The fraction of [^{11}C]**1** (rt: 44-50 min) was diluted with 150 mL water for injection and passed through a C18 SepPak®-cartridge. The cartridge was washed with 5 ml water. [^{11}C]**1** was eluted with 2 mL ethanol into 10 mL saline in 25% radiochemical yield (decay-corrected) in 99% radiochemical purity and with a specific radioactivity of 1 GBq/µmol within 91 min from the end of radionuclide production.

In conclusion, a nonpeptidyl ^{11}C-labeled caspase inhibitor, [^{11}C]**1**, was synthesized for the first time as putative CbR for the exclusive *in vivo* detection of apoptosis.

References

1. Lahorte CMM et. al. *Eur J Nucl Med Mol Imaging* 2004; **31**: 887-919.
2. Lee D et al. *J Biol Chem* 2000; **275**: 16007-14.
3. Chapman JG et al. *Eur J Pharmacol* 2002; **456**: 59-68.
4. Kopka et al. Patent application, EP 05000828.3, *5-Pyrrolidinylsulfonyl isatin derivatives*, filed 01/17/2005.
5. Lee D et al. *J Med Chem* 2001; **44**: 2015-2026.

Keywords: Caspase Inhibitor, Nonpeptidyl, 5-Pyrrolidinylsulfonyl Isatin, Carbon-11, Synthesis

CASPASE-3 SUBSTRATES AS POTENTIAL APOPTOSIS IMAGING AGENTS

C. Bauer,[1] U. Bauder-Wuest,[1] W. Mier,[2] U. Haberkorn,[2] M. Eisenhut.[1]
[1]Department of Radiopharmaceutical Chemistry, German Cancer Research Center, Heidelberg, Germany; [2]Department of Nuclear Medicine, University of Heidelberg, Heidelberg, Germany.

Objectives: Apoptosis imaging with ^{99m}Tc-HYNIC-annexin V is based on the binding of the tracer to externalized phosphatidyl serine. This compound is currently tested for monitoring lung cancer therapy. Concurrently with the externalization of phosphatidyl serine a series of caspases are activated after the onset of apoptosis. These enzymes were chosen as an alternative target for apoptosis imaging. The aim of this project was focussed on the development and investigation of peptides serving as substrates for caspase-3, one of the main executioner proteases in apoptosis.

Methods: One requirement of the peptides serving as caspase-3 substrates is the specific recognition sequence DEVD. A series of peptides containing this sequence was synthesized by solid phase synthesis using *N*-α-Fmoc protected amino acids and HBTU as a coupling reagent. All peptides were cleaved from the resin as *C*-terminal amides. Radiolabeling was carried out with ^{131}I and in subsequent experiments with ^{99m}Tc. Cell uptake studies were performed using normal controls and apoptotic Jurkat cells. The substrate specificity of two peptides, YDEVDG-NH_2 and Tat_{49-57}-yDEVDG-NH_2, was investigated with recombinant caspase-3 and with lysate of apoptotic cells.

Results: In vitro time course experiments of the radioiodinated peptides DEVDGY-NH_2, YDEVDG-NH_2, NQVNGY-NH_2 and YNQVNG-NH_2 revealed no uptake preference in apoptotic cells. To achieve an increase in cellular uptake these peptides were combined with the transporter peptide Tat_{49-57} and its reversed sequence Tat_{57-49}. Two of six peptides investigated here, Tat_{49-57}-yDEVDG-NH_2 and Tat_{57-49}-yDEVDG-NH_2, showed preferential uptake in apoptotic cells (Fig. 1). Compared with the former peptide the ^{99m}Tc complexes obtained with Tat_{49-57}-C(Acm)GC(Acm)DEVDG-NH_2 demonstrated also higher uptake in apoptotic cells (Fig. 2). Differences in cell uptake behaviour of the two isomeric forms resulting from this reaction illustrate the sensitive sterical requirements for being transportet and/or accepted by the enzymes. Proof of caspase-3 substrate specificity was received with Tat_{49-57}-yDEVDG-NH_2 by a competitive caspase-3 assays and MALDI-MS.

Conclusions: Within the series DEVDG derivatives the radiolabeled peptides obtained with Tat_{49-57}-yDEVDG-NH_2, Tat_{57-49}-yDEVDG-NH_2 and Tat_{49-57}-C(Acm)GC(Acm)DEVDG-NH_2 were found to exhibit significant uptake differences in favour of apoptotic cells. The enhanced retention is interpreted with the interaction of the labelled peptide or peptide fragment with activated caspases. Animal experiments are planned in due course.

Financial Support of the FP6 Program (EMIL) of the European Union is greatfully acknowledged.

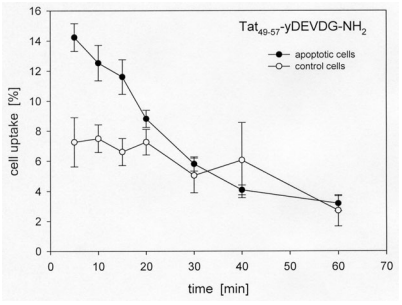

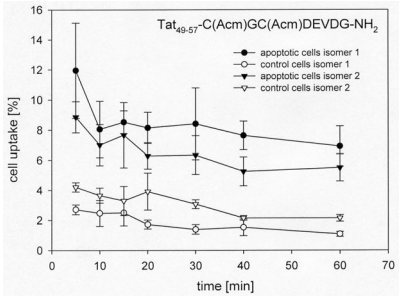

Keywords: Caspase Substrates, Radiolabeled Peptides, Cell Uptake

SYNTHESIS AND *IN VITRO* EVALUATION OF ^{111}In-DOTA-anti-*bcl-2*-PNA-Tyr^3-OCTREOTATE IN CHRONIC LYMPHOCYTIC LEUKEMIA CELLS

F. Jia,[1] F. Gallazzi,[2] S.Z. Lever,[3] M. Hannink,[4] M.R. Lewis.[1]
[1]Department of Veterinary Medicine and Surgery, University of Missouri-Columbia; [2]Molecular Biology Program; [3]Department of Chemistry; [4]Department of Biochemistry.

The *B-cell lymphoma/leukemia-* 2 (*bcl-2*) gene produces an apoptosis inhibitor overexpressed by many cancers. The purpose of this study was to synthesize and evaluate radiolabeled peptide nucleic acid (PNA)-peptide conjugates targeting *bcl-2* gene expression. We previously reported ^{111}In-labeled anti-*bcl-2*-PNA conjugated to a cell-penetrating peptide, PTD-4 (1, 2). In this study, we replaced the non-specific PTD-4 with a somatostatin receptor ligand, to improve the tumor targeting specificity of the PNA conjugate.

DOTA-anti-*bcl-2*-PNA-Tyr^3-octreotate was synthesized by standard solid-phase Fmoc chemistry. ^{111}In-DOTA-anti-*bcl-2*-PNA-Tyr^3-octreotate (**1**) was purified and separated from unlabeled conjugate by RP-HPLC. The binding specificity of **1** was determined by Northern blotting with bcl-2 and luciferase mRNAs. Uptake and blocking studies of **1** and ^{111}In-DOTA-Tyr^3-Octreotate (**2**) were performed in the chronic lymphocytic leukemia (CLL) cell line Mec-1, which expresses both somatostatin receptors and bcl-2 mRNA. For blocking experiments, excess unlabeled DOTA-Tyr^3-octreotate was added simultaneously with the radiopharmaceuticals.

HPLC retention times were 22.2 min for **1** and 22.7 min for the unlabeled conjugate. Compound **1** could be labeled to extremely high specific activity with up to 90% incorporation of ^{111}In and 100% radiochemical purity. Northern blot analysis showed that **1** bound specifically to as little as 5 ng (50 fmol) of bcl-2 mRNA, while no binding to the luciferase transcript was observed. From 1-60 min, uptake of **1** in Mec-1 cells was 1.27-2.62% of the total radioactivity added, and this value increased significantly to 3.97% at 120 min and 5.16% at 240 min (Table 1). Mec-1 cell uptake of **1** was approximately twice that of **2**. Blocking studies reduced cellular accumulation to ≤1% for both compounds. Western blot studies will be presented to assess cellular bcl-2 mRNA targeting.

In conclusion, a new tumor-specific PNA-peptide conjugate to target *bcl-2* gene expression was prepared and labeled with ^{111}In at specific activities sufficient for *in vivo* antisense imaging. This ^{111}In-labeled PNA-peptide conjugate showed high sensitivity, high specificity bcl-2 mRNA binding in a cell-free system and somatostatin-receptor mediated CLL cell uptake. It will be evaluated for SPECT imaging of tumor *bcl-2* expression in mouse models of CLL.

Acknowledgments: This work was supported by NIH Grant CA103130 from the National Cancer Institute. We would like to thank Dr. Charles W. Caldwell for providing the Mec-1 cell line.

References:

1. Lewis, M.R., *et al.*, *J. Labelled Cpd. Radiopharm.* **46:** S13 (2003).

2. Gallazzi, F., *et al.*, *Bioconjugate Chem.* **14:** 1083-1095 (2003).

Table 1. Uptake and Blocking (mean ± s.d., n = 3) of In-111-DOTA-anti-bcl-2-PNA-Tyr-3-octreotate (1) and In-111-DOTA-Tyr-3-octreotate (2) in Mec-1 cells

Time (min)	1 Uptake (%)	1 Block (%)	2 Uptake (%)	2 Block (%)
1	2.25 ± 0.20	0.91 ± 0.00	0.51 ± 0.13	0.51 ± 0.06
5	1.27 ± 0.016	1.07 ± 0.16	0.72 ± 0.40	0.44 ± 0.19
15	1.41 ± 0.02	0.93 ± 0.02	1.21 ± 0.12	0.39 ± 0.09
30	2.62 ± 0.02	1.09 ± 0.04	1.26 ± 0.37	0.32 ± 0.02
60	2.58 ± 0.14	0.58 ± 0.07	1.62 ± 0.19	0.30 ± 0.09
120	3.97 ± 0.36	0.76 ± 0.05	1.92 ± 0.14	0.26 ± 0.02
240	5.16 ± 0.42	0.73 ± 0.02	2.58 ± 0.07	0.24 ± 0.01

Keywords: Peptide Nucleic Acid, Bcl-2, Leukemia/Lymphoma

SYNTHESIS AND BIOLOGICAL EVALUATION OF RADIOLABELED $\alpha_v\beta_3$ INTEGRIN RECEPTOR ANTAGONISTS

I. Dijkgraaf,[1] P. Laverman,[1] R.M. Liskamp,[2] O.C. Boerman.[1]
[1]*Department of Nuclear Medicine, Radboud University Nijmegen Medical Center, Nijmegen, Netherlands;*
[2]*Department of Medicinal Chemistry, Utrecht Institute for Pharmaceutical Sciences, Utrecht University, Utrecht, Netherlands.*

Objectives: The $\alpha_v\beta_3$ integrin is expressed on sprouting endothelial cells but is absent on quiescent endothelial cells. In addition, $\alpha_v\beta_3$ is expressed on various tumor types. This integrin can bind to the arginine-glycine-aspartic acid (RGD) sequence of extracellular matrix proteins such as vitronectin. Here, we present the synthesis of three ligands based on this RGD tripeptide sequence and their conjugation with 1,4,7,10-tetraazadodecane-N,N′,N″,N‴-tetraacetic acid (DOTA): (1) the cyclic pentapeptide DOTA-E-c[RGDfK] and, (2) the cyclic peptoid-peptide hybrid DOTA-E-c[nRGDfK] and, (3) a nonpeptide integrin $\alpha_v\beta_3$ receptor antagonist. In the peptoid-peptide hybrid arginine is replaced by the corresponding peptoid residue. In peptoid residues, the position of the amino acid side chain is shifted from the α-carbon atom to the nitrogen atom making peptoids less sensitive to proteolytic degradation. The nonpeptide compound was based on a recently described peptidomimetic (Hood *et al*., Science, 2002;296:2404-2407). The radiolabeling, metabolic stability and the in vivo tumor targeting characteristics of these compounds were investigated.

Methods: The peptide and the peptide-peptoid hybrid were synthesized using Fmoc based solid phase peptide synthesis. All compounds were conjugated with DOTA using DOTA-tris(*tert*Bu). ^{111}In labeling was performed in ammoniumacetate buffer with gentisic acid at 100°C for 15 minutes. The radiochemical purity was determined by RP-HPLC. The stability of the ^{111}In-labeled compounds was determined by incubation in human serum or PBS at 37°C. Samples were analyzed on RP-HPLC. The affinity of the compounds for $\alpha_v\beta_3$ integrin was studied using a competitive solid-phase receptor binding assay using ^{111}In-DOTA-E-$[c(RGDfK)]_2$ as a tracer. Biodistribution and tumor targeting was studied in nude mice bearing s.c. human ovarian carcinoma (IGROV1) tumors (n=4 mice/group).

Results: All compounds could be labeled with ^{111}In with a radiochemical purity > 95%. Stability tests revealed good stability of the ^{111}In-DOTA-E-c[RGDfK] and ^{111}In-DOTA-E-c[nRGDfK] after incubation for 6 h in human serum. However, the ^{111}In-nonpeptide was slowly degraded over time, with 50% of the initial labeled compound remaining after 6 h in serum. The IC_{50} values were 236 nM for DOTA-E-c[RGDfK], 9.25 mM for DOTA-E-c[nRGDfK], and 219 nM for the nonpeptide. The in vivo study revealed a rapid blood clearance of all three compounds. At 2 hours p.i., blood levels were 0.02 ± 0.00 %ID/g, 0.02 ± 0.00%ID/g, and 0.07 ± 0.01 %ID/g (c[RGDfK], c[nRGDfK], nonpeptide, respectively). Tumor uptake of the nonpeptide (2.26 ± 0.22 %ID/g) was higher than that of ^{111}In-DOTA-E-c[RGDfK] (1.47 ± 0.28 %ID/g) and ^{111}In-DOTA-E-c[nRGDfK] (0.45 ± 0.07 %ID/g). Uptake in all other tissues was lower than tumor uptake (except for the kidney uptake of ^{111}In-DOTA-E-c[nRGDfK]). Tumor accumulation could be blocked by coinjection of an excess of unlabeled compound. Specific uptake was also noted in stomach, liver, spleen, colon and small intestine, indicating $\alpha_v\beta_3$ integrin expression in these organs.

Conclusions: Three different $\alpha_v\beta_3$ binding ligands were synthesized and conjugated with DOTA. All compounds showed specific uptake in $\alpha_v\beta_3$-expressing IGROV1 tumors. The nonpeptide had the highest tumor uptake, whereas the peptoid-peptide hybrid showed the lowest uptake in this model. This correlated with their IC_{50} values as determined on the $\alpha_v\beta_3$ integrin in vitro. The replacement of arginine by its peptoid monomer did not improve serum stability and negatively affected the affinity for the $\alpha_v\beta_3$ integrin.

Keywords: Peptide, Angiogenesis, Peptidomimetics

AN EASY METHOD FOR NO-CARRIER-ADDED ^{18}F-LABELING OF RGD PEPTIDE: HYDRAZONE FORMATION BETWEEN cRGDyK-HYNIC AND 4-[^{18}F]FLUOROBENZALDEHYDE (FBA)

Y.-S. Lee,[1] J.M. Jeong,[1] H.W. Kim,[1] Y.S. Chang,[1] B.R. Ganasha,[1] Y.-G. Suh,[2] D.Y. Chi,[3] W.J. Kang,[1] J.H. Kang,[1] D.S. Lee,[1] J.-K. Chung,[1] M.C. Lee.[1]

[1]Department of Nuclear Medicine, College of Medicine, Seoul National University, Seoul, Republic of Korea; [2]Department of Manufacturing Pharmacy, College of Pharmacy, Seoul National University, Seoul, Republic of Korea; [3]Department of Chemistry, Inha University, Inchon, Republic of Korea.

The importance of radiolabeled a_vb_3-integrin antagonists is increasing for imaging tumor-associated angiogenesis[1]. Several methods of ^{18}F labeling of the a_vb_3-integrin adhesion receptor have recently been developed[2,3,4]. We developed a new method for ^{18}F labeling of RGD peptide via a hydrazone formation reaction between cRGDyK- hydrazinonicotinic acid (HYNIC) conjugate and 4-[^{18}F]fluorobenzaldehyde (FBA).

cRGDyK-NH_2 was coupled with HYNIC *N*-hydroxysuccinic anhydride ester (NHS-HYNIC) in the basic buffer solution and the reaction mixture was purified with preparative HPLC to give cRGDyK-HYNIC[5,6]. The structure of the compound was confirmed by ^{1}H-NMR and Mass spectroscopy. 4-[^{18}F]FBA was produced using a known method[7]. cRGDyK-HYNIC and 4-[^{18}F]FBA were coupled in the acidic buffer solution (pH=4.5) at 80° for 30 min, and the reaction mixture was purified with preparative HPLC (Waters, Xterra RP8, 10 x 250 mm; from 20% EtOH/water to 50% EtOH/water over 20 min; 3 mL/min) to give [^{18}F]fluorobenzylidenehydrazone-nicotinamide-cRGDyK ([^{18}F]FBHNA-cRGDyK). HYNIC and 4-[^{18}F]FBA conjugate was also prepared with the same condition for comparison. The labeling efficiency was checked by radio TLC (eluted by 25% ethyl acetate/*n*-hexane on silica gel) and the radiochemical purity was checked by an analytical HPLC (BioRad, Rsil C18HL, 4.6 x 150 mm; from 5% EtOH/water to 80% EtOH/water over 20 min; 1 mL/min).

The purity of cRGDyK-HYNIC was above 99%. The labeling efficiency of 4-[^{18}F]FBA was 40.1±12.9 % (n=3), and the radiochemical purity after purification was over 99%. The labeling efficiencies of [^{18}F]FBHNA-cRGDyK and [^{18}F]fluorobenzylidenehydrazone-nicotinic acid ([^{18}F]FBHNA) were 30.2% and 96.4%, respectively. The radiochemical purities of [^{18}F]FBHNA-cRGDyK and [^{18}F]FBHNA were >99% (t_{Ret} = 8.4 min) and 96% (t_{Ret} = 9.3min), respectively. Total synthesis time was 140 min after irradiation.

We developed a new method for no-carrier-added ^{18}F labeling of RGD peptide via a hydrazone formation reaction between cRGDyK-HYNIC conjugate and 4-[^{18}F]FBA.

References

1. Boerman OC, Oyen WJ, and Corstens FH, *Semin Nucl Med*, 2000;30: 195–208.
2. Haubner R, Wester HJ, Weber WA, Mang C, Ziegler SI, Goodman SL, Senekowitsch-Schmidtke R, Kessler H, Schwaiger M, *Cancer Res,* 2001;61:1781-1785.
3. Poethko T, Schottelius M, Thumshirn G, Hersel U, Herz M, Henriksen G, Kessler H, Schwaiger M, Wester HJ, *J Nucl Med*, 2004;45:892-902.
4. Chen X, Park R, Shahinian AH, Tohme M, Khankaldyyan V, Bozorgzadeh MH, Bading JR, Moats R, Laug WE, Conti PS, *Nucl Med Biol*, 2004;31:179-89.
5. Abrams MJ, Juweid M, tenKate CI, Schwartz DA, Hauser MM, Gaul FE, Fuccello AJ, Rubin RH, Strauss HW and Fischman AJ, *J Nucl Med*, 1990;31:2022–2028.
6. Schwartz DA, Abrams MJ, Hauser MM, Gaul FE, Larsen SK, Rauh D, and Zubieta JA, *Bioconjugate Chem,* 1991;2:333-336
7. Haka MS, Kilbourn MR,Watkins GL, Toorongian SA, *J Label Compd Radiopharm* 1989; 27:823–833.

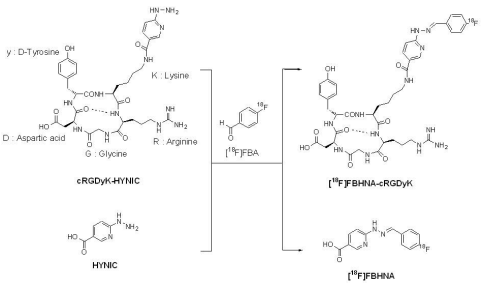

Keywords: Integrin, RGD Peptide, HYNIC

SYNTHESIS OF FLUORINE-18 LABELED GLUCOSE-Lys-Arg-Gly-Asp-D-Phe AS A POTENTIAL TUMOR IMAGING AGENT

J.S. Kim,[1] K.C. Lee,[2] B.C. Lee,[1] B.S. Moon,[2] H.J. Song,[1] K.S. Chun,[2] D.Y. Chi.[1]
[1]Department of Chemistry, Inha University, Inchon, Republic of Korea; [2]Laboratory of Radiopharmaceuticals, Korea Institute of Radiological and Medical Sciences, Seoul, Republic of Korea.

As $\alpha_v\beta_3$ integrin is expressed on proliferating endothelial cells as well as on tumor cells of various origin, tumor-induced angiogenesis could be blocked by antagonizing the $\alpha_v\beta_3$ integrin with RGD. Therefore, $\alpha_v\beta_3$ integrin is a target for angiogenesis imaging that might be useful in assessing tumor-induced angiogenesis and identifying tumor metastasis. To design potent radiotracer for imaging angiogenesis containing a cRGD moiety should include low hepatic uptake in vivo [1].

Our interest in developing new radiopharmaceuticals for in vivo visualization of angiogenesis has led us to synthesize derivatives of cRGD (cyclic arginine-glycine-aspartic acid) that contains glucose moiety. Because sugar-protein interaction is a key step in metastasis and angiogenesis [2], it has also been proposed to play an intriguing role in imaging of tumor.

We designed and synthesized two fluorine-18 labeled RGD glycopeptides – *N*-fluorobenzyl-diaminobutane-*N′*-glucose-Lys-Arg-Gly-Asp-D-Phe ([^{18}F]fluorobenzyl-glucose-KRGDf, **1**) and *N*-fluorobenzoyl-diaminobutane-*N′*-glucose-Lys-Arg-Gly-Asp-D-Phe ([^{18}F]fluorobenzoyl-glucose-KRGDf, **2**) from same precursor as a diagnostic tumor imaging agent for positron emission tomography (PET). Fluorine-18 labeled cRGD glycopeptides were prepared using two different simple labeling methods: one is reductive alkylation of an amine with [^{18}F]fluorobenzaldehyde and the other is amide condensation with [^{18}F]fluorobenzoic acid.

[^{18}F]Fluorobenzyl-glucose-KRGDf **1** and [^{18}F]fluorobenzoyl-glucose-KRGDf **2** were prepared in 10-15 and 20% radiochemical yields, respectively, and then purified by HPLC at a flow rate of 2 mL/min (20-60% CH_3CN/0.1% TFA in H_2O, 30 min). The desired fraction eluted at 13.4 and 15.8 min was collected and matched with cold compound. The radiolabeling conditions are currently being optimized, and in vivo studies are in progress.

1. Haubner R, Wester H-J, Weber WA, Mang C, Zigler SI, Goodman SL, Senekowitsch-Schmidtke R, Kessler H, Schwaiger M. *Cancer Res* 2001; 61: 1781-1785.
2. Muramatsu T. *Glycobiology* 1993; 3: 291-296.

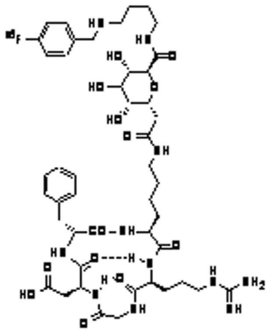

[^{18}F]fluorobenzyl-glucose-KRGDf **1**

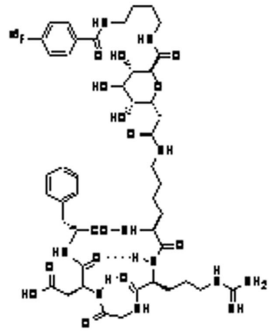

[^{18}F]fluorobenzoyl-glucose-KRGDf **2**

Keywords: $\alpha_v\beta_3$ Integrin, Integrin Binding Peptide, cRGD

SYNTHESIS AND BIODISTRIBUTION OF $^{99m}Tc(CO)_3$-TRIDENTATE-LABELED INTEGRIN ANTAGONIST IN TUMOR BEARING MICE

S.H. Park,[1] B.S. Jang,[1] E. Lim,[2] M. Bur,[2] J. Xie,[2] N. Le,[1] N. Danthi,[2] M. Dewanjee,[2] K.C. Li,[2] J.A. Carrasquillo,[1] C.H. Paik.[1]

[1]Nuclear Medicine, Clinical Center of National Institutes of Health, Bethesda, MD, United States; [2]Radiology, Clinical Center of National Institutes of Health, Bethesda, MD, United States.

Objectives: Selective targeting of integrin $\alpha_v\beta_3$ receptor with radioligands may enable assessment of angiogenesis and receptor status in tumors. The aim of this research was to label a peptidomimetic integrin $\alpha_v\beta_3$ antagonist, 4-[2-(3,4,5,6-tetrahydro-pyrimidine-2-ylamino)ethyloxy]benzoyl-2-(S)-aminoethylsulfonylamino-β-alanine (IA) with ^{99m}Tc $(CO)_3$ using *tris*-succinimidyl aminotriacetate (TSAT) as a bifunctional chelator, and test its receptor targeting properties in nude mice bearing receptor-positive tumor. **Methods:** We optimized reaction conditions to acylate the amino group of IA with one of the three activated esters of TSAT and to hydrolyze the remaining two esters to produce an aminodiacetic acid moiety: IA was reacted with TSAT (20 mM) at an IA to TSAT molar ratio ranging from 1.2:1 to 5:1 at pH 8.5 for 1 hr at room temperature. The product IA-$COCH_2N(CH_2CO_2H)_2$ (IA-ADA) was reacted with $[^{99m}Tc(CO)_3(H2O)_3]^{+1}$ at pH 4.5 for 45 min at 70°C, and purified sequentially on Sep-Pak C-18 and Sep-Pak QMA anion exchange cartridges. The radiochemical purity (>95%) of Tc-99m (CO)3 ADA-IA (retention time, 10.5 min) was confirmed by gradient C-18 reverse-phase HPLC. The stability was tested against histidine (20 mM in PB at pH 7.2) at a 200 times molar excess to the Tc-99m label at 37°C. The biodistribution was performed in nude mice (n =5 per time point) bearing receptor-positive M21 human melanoma xenografts. The mice received *i.v.* ^{99m}Tc $(CO)_3$ ADA-IA (5 mCi/<0.1 mg in 0.2 ml of PBS containing 1% BSA). The animals were euthanized at 0.33, 1 and 2 hr after injection for the biodistribution study. A group of mice was also coinjected with 200 mg of IA and was euthanized at 1 hr to test if the tumor uptake is blocked with the excess amount of IA. **Results:** The conjugation reaction of IA to TSAT at a molar ratio of 1.2:1 produced a higher yield of mono IA conjugated to TSAT as compared to the reaction at an IA to TSAT molar ratio of 5:1. ^{99m}Tc $(CO)_3$ ADA-IA was stable in PB for 21 hr, but lost 7.9 and 11.5 of the radioactivity to histidine at 3 and 6 hr. Since the labeled product was quite stable for 3 hr in the harsh trans-chelation condition, we undertook biodistribution studies. In the tumor bearing mice, it accumulated rapidly in the receptor-positive tumor with a peak uptake of 1.2 ± 0.4% ID/g at 20 min, while being cleared rapidly from blood primarily via the hepatobiliary system with 6.5 ± 0.8 and 25.4 ± 2.8% ID/g localized in liver and intestine, respectively at that time. At 20 min, the tumor to organ ratios were 1.8, 0.18, 0.69, 1.0, 2.9, 0.22, 0.04, 2.1 and 4.1 for blood, liver, kidney, lung, heart, stomach, intestine, bone and muscle, respectively. At 1 hr, the tumor uptake was 0.47 ± 0.15% ID/g, but decreased to 0.12 ± 0.02% ID/g when coinjected with the excess amount of IA, indicating that it accumulated by receptor mediated uptake. However, the tumor to organ ratios did not improve much over time because the labeled IA was not retained well in the tumor perhaps due to its low affinity to the receptor. **Conclusion:** A peptidomimetic antagonist to integrin was successfully labeled with ^{99m}Tc. It accumulated in the tumor mediated via specific receptor binding. This study suggests that to be useful as a tumor detection agent, it is necessary to improve the receptor-binding affinity by synthesizing oligomers of IA and also to increase hydrophilicity of the product by glycosylation and PEGylation to minimize the rapid uptake into the hepatobiliary system.

Keywords: Tumor Detection, Receptor-Binding Radiopharmaceutical, Technetium-99m Tricarbonyl

SYNTHESIS AND *IN VITRO* BINDING AFFINITY OF PEGYLATED MULTIDENTATE cRGDyK PEPTIDE

Y.-S. Lee, J.M. Jeong, M.K. Hong, Y.S. Chang, B.R. Ganesha, W.J. Kang, J.H. Kang, D.S. Lee, J.-K. Chung, M.C. Lee.
Department of Nuclear Medicine, Seoul National University College of Medicine, Seoul, Republic of Korea.

The $\alpha_v\beta_3$ integrin plays an important role in angiogenesis[1], and cyclic RGD (Arg-Gly-Asp) peptide has high affinity and selectivity for the $\alpha_v\beta_3$ integrin. However, cRGD itself revealed fast hepatobiliary excretion[2,3]. In view of a recent report that pharmacokinetics and tumor retention of ^{125}I-labeled RGD peptide are improved by PEGylation[4], we have coupled di-, tetra-, hexa-armed PEG with cRGDyK and investigated the *in vitro* $\alpha_v\beta_3$ integrin affinities.

Terminal amino groups were introduced to di-, tetra-, hexa-armed PEG's (M.W. 20K) and were modified with succinic anhydride. The resulting terminal acid groups were activated with 2-(1*H*-benzotriazol-1-yl)-1,1,3,3-tetramethyluronium tetrafluoroborate (HBTU) and 1-hydroxybenzotriazole (HOBt), and coupled with protected cRGDyK-NH_2 using *N,N*-diisopropylethylamine (DIEA) as a base[5,6]. The products were deprotected with trifluoroacetic acid and purified with PD10 column to give bis(cRGDyK)-PEG, tetrakis(cRGDyK)-PEG and hexakis(cRGDyK)-PEG. The cRGDyK was labeled with ^{125}I using the chloramine-T method, and subsequently purified by HPLC using a reverse-phase column eluted with a mixture of ethanol and 0.01% TFA in water. The $\alpha_v\beta_3$integrin was purified from human placenta using affi-gel coupled with cRGDyK. The Kd value of ^{125}I-cRGDyK was evaluated with $\alpha_v\beta_3$ integrin coated polystyrene well plate. The binding affinities of PEGylated cRGDyK were evaluated for competition against ^{125}I-cRGDyK binding to $\alpha_v\beta_3$ integrin.

The labeling efficiency of ^{125}I-cRGDyK was 92.8%, radiochemical purity after purification was over 99% and specific activity was 2.175Í10^6 Ci/mol. The Kd values of ^{125}I-cRGDyK was 1.013 nM. The Ki values of cRGDyK, bis(cRGDyK)-PEG, tetrakis(cRGDyK)-PEG and hexakis(cRGDyK)-PEG were 44.64, 873.5, 457.8, and 100.4 nM, respectively.

We synthesized PEG linked multidentate RGD peptide, bis(cRGDyK)-PEG, tetrakis(cRGDyK)-PEG and hexakis(cRGDyK)-PEG. As the number of cRGD peptides conjugated to the PEG increased, the binding affinity to$\alpha_v\beta_3$ integrin was also increased.

References
1. Ingber D, *J Cell Biochem* 1991;47:236–41.
2. Haubner R, Reuning U, Senekowitsch-Schmidtke R, Diefenbach B, Kessler H, Stocklin G, Schwaiger M, *J Nucl Med* 1999;40:1061–71.
3. Haubner R, Wester H-J, Burkhart F, Senekowitsch-Schmidtke R, Weber W, Goodman SL, Kessler H, and Schwaiger M, *J Nucl Med* 2001;42:326–36.
4. Chen X, Park R, Shahinian AH, Bading JR, Conti PS, *Nucl Med and Biol* 2004;31:11–19
5. Dourtoglou V, Gross B, Lambropoulou V, Zioudrou C, *Synthesis* 1984;572
6. Klausner Y, Bodansky M, *Synthesis* 1972;453

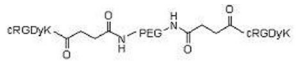

Bis(cRGDyK)-PEG

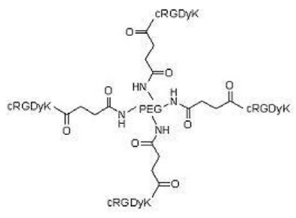

Tetrakis(cRGDyK)-PEG

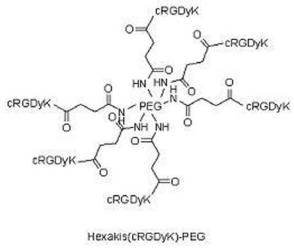

Hexakis(cRGDyK)-PEG

Keywords: $\alpha_v\beta_3$ Integrin, RGD Peptide, PEG

SYNTHESIS AND EVALUATION OF 4-[^{18}F]FLUOROTHALIDOMIDE FOR THE *IN VIVO* STUDIES OF ANGIOGENESIS

D.H. Kim, Y.S. Choe, K.H. Jung, K.H. Lee, Y. Choi, B.T. Kim.
Nuclear Medicine, Samsung Medical Center, Sungkyunkwan University School of Medicine, Seoul, Korea.

Thalidomide has been recently reilluminated as an antitumor agent, although it was marketed as a sedative in the 1950s and later found to be a potent teratogen. It was shown that thalidomide has the antiangiogenic effect by inhibiting the activated endothelial cells, but its mechanism is not fully understood. Currently, thalidomide is being tested in Phase II clinical trials in prostate, breast, brain and skin cancers. In this study, ^{18}F-labeled thalidomide was synthesized and evaluated for the in vivo studies of angiogenesis.

4-Fluorothalidomide, a cold standard, was synthesized from 4-fluorophthalic anhydride and glutarimide in acetic acid. 4-[^{18}F]Fluorothalidomide ([^{18}F]**1**) was prepared by labeling of 4-trimethylammoniumthalidomide trifluoromethanesulfonate with ^{18}F in DMSO (95 °C, 10 min). 4-Trimethylammonium triflate precursor was synthesized by refluxing 4-fluorothalidomide with dimethylamine HCl, followed by reacting with methyl trifluoromethanesulfonate ester. The radiolabeled reaction mixture was purified by reverse phase HPLC and the desired fraction was collected for biological evaluation. Radiochemical yield was 50-60%. 4-Nitrothalidomide prepared from 4-nitrophthalic anhydride and glutarimide was also used as the precursor for ^{18}F-labeling, which required harsh labeling conditions (150-160 °C, 30 min) and gave the product in low radiochemical yield (12%).

[^{18}F]**1** (10 μCi/5 μL) was dissolved in saline containing 1% DMSO (final concentration 0.02%) and incubated with HUVEC (human umbilical vein endothelial cells) at 37 °C for 15, 30, 60, and 120 min. At the indicated time points, the cells were washed with PBS containing 0.1% bovine serum albumin to prevent non-specific binding and then counted. The cell uptake of [^{18}F]**1** increased in a time-dependent manner: 133% at 30 min, 170% at 60 min, and 240% at 120 min relative to 100% at 15 min. In the presence of 10 μM thalidomide, [^{18}F]**1** uptake to HUVEC at 60 min was inhibited by 11%. Dynamic PET images of [^{18}F]**1** was obtained in mice (C57BL6) implanted with Lewis lung carcinoma cells at the right flank. High radioactivity accumulation was detected in the liver, kidneys and bladder, and the brain uptake started to appear at 40 min postinjection. However, there was low radioactivity uptake in tumor. In order to investigate the metabolic activation, [^{18}F]**1** was incubated with mouse liver microsomes (0.25 mg/ml) in the presence of NADPH (0.25 mM) at 37 °C. Radiometabolites were not detected on radio-TLC, indicating that [^{18}F]**1** was not metabolized by mouse liver microsomes. This result was consistent with those of the literatures in that the activation of thalidomide may be responsible for its antiangiogenic effect and that the activation occurs by human and rabbit liver microsomes but not by rodent microsomes. Low level of inhibition of the radioactivity uptake by thalidomide and low radioactivity accumulation in tumor on the right flank suggested that the activation of [^{18}F]**1** may be required for the in vivo studies of angiogenesis.

In conclusion, this result demonstrated that [^{18}F]**1** might not be activated in mice, and therefore further studies are warranted to carry out the in vivo studies in rabbits in which thalidomide is known to be activated by the liver enzymes.

Keywords: 4-[Fluorine-18]fluorothalidomide, Angiogenesis, PET

LABELING AND BIODISTRIBUTION OF AN ANGIOGENIN INHIBITOR IDENTIFIED BY HIGH THROUGHPUT SCREENING

W. Mier,[1] J. Hoffend,[1] M. Eisenhut,[2] U. Haberkorn.[1]
[1]Nuklearmedizin, Universitatsklinikm Heidelberg, Heidelberg, Germany; [2]Radiopharmazeutische Chemie, Deutsches Krebsforschungszentrum, Heidelberg, Germany.

Angiogenin (ANG) is a potent inducer of angiogenesis. This protein is a 14.1 kDa member of the pancreatic RNase superfamily and was demonstrated to play a critical role in the angiogenesis of growing tumors. Recently, the identification of a low molecular weight compound that binds to the ribonucleolytic active site of ANG has attracted strong attention. This compound has been identified by high-throughput screening from a library comprising 18,310 low molecular weight substances (1). Here we report the design and biodistribution of a radiolabeled derivative of this compound which might be used as a lead compound for both diagnostic and endoradiotherapeutic applications.

The ANG inhibitor 8-Amino-5-(4′-hydroxy-biphenyl-4-ylazo)-naphthalene-2-sulfonic acid (1) was iodinated with 131-I using the potassium iodate method to yield 8-Amino-5-(4′-hydroxy-3′-[131-I]iodo-biphenyl-4-ylazo)-naphthalene-2-sulfonic acid. The biodistribution of the radiolabeled compound was determined in mice bearing either PC-3 or HT-29 tumors. Biodistribution data were obtained at four time points and a competition experiment using the cold ANG inhibitor was performed.

The labeling procedure turned out to be complicated due to solubility limitations. However, of the several methods examined, the potassium iodate method enabled the formation of the iodinated derivative in high yield and regioselectivity. The biodistribution in mice revealed an unfavorable behavior of this compound in vivo: an almost exclusive uptake in the liver was observed at 5 and 15 min p.i. in both tumor models. Tumor uptake values were lower than 0.1 %ID/g in both tumor models at all of the time points investigated.

The recent advances in assay and instrument technologies have provided the means for the high throughput screening. However, the screening methods identify compounds depending on factors such as potency of an enzyme inhibitor or the binding affinity of a receptor ligand. Other factors, in particular the pharmacokinetics are not sufficiently considered when choosing the novel pharmaceutical leads. This study reveals an example that the success of novel therapeutics is doomed if pharmacokinetics are not considered in the early stages of drug design.

(1) Kao RY, Jenkins JL, Olson KA et al. A small-molecule inhibitor of the ribonucleolytic activity of human angiogenin that possesses antitumor activity. Proc Natl Acad Sci U S A. 99 10066 (2002).

Keywords: Angiogenin Inhibitor, Biodistributon, Iodination

EVALUATION OF [F-18]IRESSA AS A PET IMAGING AGENT FOR TUMORS OVEREXPRESSING EPIDERMAL GROWTH FACTOR (EGF) RECEPTORS

D. Murali,[1] L.G. Flores,[1] A.K. Converse,[2] R.M. Bartlett,[1] T.E. Barnhart,[1] E.A. Armstrong,[3] R.J. Nickles,[1] P.M. Harari,[3] O.T. DeJesus.[1]

[1]Medical Physics, University of Wisconsin Medical School, Madison, WI, United States; [2]W. M. Keck Laboratory for Brain Imaging, University of Wisconsin Waisman Center, Madison, WI, United States; [3]Human Oncology, University of Wisconsin Medical School, Madison, WI, United States.

Epidermal growth factor receptors (EGFR) are epithelial cell membrane receptors with intracellular tyrosine kinase (TK) domain involved in cell signaling functions critical in mitogenesis, cell proliferation, differentiation, and angiogenesis. Two-thirds of cancers derive from epithelial tissues and EGFR-TK is overexpressed in many of these tumors. In recent years several EGFR-TK inhibitors with nanomolar affinities have been developed as potential anti-cancer drugs. Iressa (ZD1839, gefitinib), a fluorine-containing anilinoquinazoline, is a potent EGFR-TK inhibitor FDA-approved for the treatment of lung cancer. The goal of this study is to evaluate [F-18]Iressa as a PET imaging agent for tumors over-expressing EGFR. PET imaging with [F-18]Iressa may be useful in identifying patients who may benefit from Iressa treatment and in monitoring progress of therapy.

[F-18]Iressa was prepared as previously reported (DeJesus et al., J. Label. Comp. Radiopharm., 46:S1, 2003). Briefly, the standard Kryptofix-K2CO3-mediated nucleophilic [F-18] exchange reaction with a 2-chloro-4-nitro-N, N, N-trimethylanilium triflate precursor was done to yield 3-chloro-4-[F-18]fluoronitrobenzene. Reduction using sodium borohydride gave 3-chloro-4-[F-18]fluoroaniline which was then condensed with previously synthesized 7-methoxy-6-(3-morpholinopropoxy)-4-chloro-quinazoline in DMF at 145°C. And finally, HPLC purification of the reaction mixture gave high purity, high specific activity [F-18]Iressa. [F-18]Iressa biodistribution studies in normal HSD-ICR mice were done by ex vivo radioassay. In vivo biodistribution studies were done using a Concorde microPET P4 scanner in normal mice and in athymic mice with EGFR-overexpressing human squamous cell carcinoma (SCC) xenografts. At the end of the 3 hr PET scan, one xenografted animal was sacrificed, dissected and ex vivo counts in several organs including the tumor were taken.

Biodistribution studies in normal HSD-ICR mice showed high [F-18]Iressa uptake in the GI tract, liver, kidneys and bladder. Plasma metabolite analysis showed temporally decreasing percentage of unchanged [F-18]Iressa declining to 52% at 3 hr postinjection. Dynamic whole-body microPET scans of these mice gave the time course of biodistribution and confirmed the ex vivo results. Radioactivity was observe to continuously increase in the liver, small intestine, kidney and tumor in the xenografted mice. Ex vivo radioassay 3 hr post-injection showed tissue to blood [F-18] ratios (on a per gram basis) to be spleen > kidney > liver ~ small intestines > lungs ~ stomach > skin > tumor > muscle. Tumor to blood ratio was 4.5, spleen to blood ratio was about 10-fold this value while brain to blood ratio was less than one.

In conclusion, these results suggest that the slow pharmacokinetics of [F-18] radioactivity in non-tumor regions may limit the use of [F-18]Iressa as a PET imaging agent to visualize EGFR-rich tumors.

Keywords: [Fluorine-18]Iressa, Epidermal Growth Factor Receptors, Epithelial Cancers

IMAGING TUMOR EXPRESSION OF PPARg WITH BROMINE-76 LABELED ANTAGONIST

H. Lee,[1] B.N. Finck,[2] M.J. Welch,[1] R.H. Mach.[1]
[1]Mallinckrodt Institute of Radiology, Washington University in St. Louis, St. Louis, MO, United States; [2]Center for Cardiovascular Research, Washington Univeristy in St. Louis, St. Louis, MO, United States.

Peroxisome proliferator activated-receptor gamma (PPARg) binds to the peroxisome receptor response element with its heterodimeric partner, retinoid X receptor, and activates downstream gene expression. Studies have shown that PPARg inhibits the cellular growth and promotes differentiation in adipocytes, monocytes and some cancer cells, such as lung, breast, colon, prostate and liposarcomas (1). PPARg agonists have been tested in clinical trials for its tumor suppression potential. It has been shown that PPARg is overexpressed in some tumor cell lines, such as breast and prostate. In contrast, the low basal expression of PPARg in the surrounding tissues makes PPARg-targeting compounds good candidates for tumor imaging. One PPARg agonist, SB213068 was previously targeted for radiolabeling with fluorine-18 but did not exhibit receptor-mediated uptake in biodistribution studies. (2). Two PPARg antagonists, 2-chloro-5-nitro-*N*-phenyl-benzamide (GW9662) and 2-chloro-5-nitro-*N*-pyridin-4-yl-benzamide (T0070907), provide a good lead for radiotracer development (3). The synthesis of the antagonists is shown in Scheme 1. The compounds with bromine substitutions at the C-2 position yield EC_{50} values of less than 5nM in whole cell screening. Both compounds were labeled with the PET nuclide, bromine-76, utilizing copper-assisted halogen exchange reaction with a production yield of 40-70%. The 2-bromo-5-nitro-*N*-phenyl-benzamide analog was selected for subsequent studies due to its superior radiolabeling yield.

A breast tumor cell line, MDA-MB-435, exhibits higher PPARg expression and was implanted in female athymic nude mice. An *in vitro* study done on plasma and whole blood at various time points showed that 40% of the compound remained intact in plasma and about 25% in whole blood sample after 30 minute incubation. Biodistribution studies were carried out at four time points, 5 minutes, 30 minutes, 2 hours and 24 hours post injection (p.i.). The ratios for the other major tissues reached peaks at 2 hours p.i., ranging from 1.6-5.0.

Compared to the biodistribution data of F-18 labeled SB213068, radiolabeled antagonists achieved better tumor/tissue ratios in most the organs. However, several concerns arose. There is a significant initial lung uptake and the reason for the high initial lung uptake is under investigation. Currently, we are also studying whether radioactive bromide ion is released out of tumor cells due to the displacement in binding pocket.

The work is supported by grants HL13851 and CA86307 from the National Institute of Health and grant ER60218 from the Department of Energy.

Reference:

1. Elisabetta Mueller, P. S., Peter Tontonoz, Ronald M. Evans, Katherine J. Martin, Ming Zhang, Christopher Fletcher, Samuel Singer, Bruce M. Spiegelman. (1998) *Molecular Cell* **1**, 465-470
2. Sung-Hoon KIm, S. D. J., Michael J. Welch, John A. Katzenellenbogen. (2001) *Bioconjugate Chem,* **12**, 439-450
3. Lisa M. Leesnitzer, D. J. P., Randy K. Bledsoe, Jeff E. Cobb, Jon L. Collins, Thomas G. Consler, Roderick G. Davis, Emily A. Hull-Ryde, James M. Lenhard, Lisa Patel, Kelli D. Plunket, Jennifer L. Shenk, Julie B. Stimmel, Christina Therapontos, Timonthy M. Willson, Steven G. Blanchard. (2002) *Biochemistry* **41**, 6640-6650

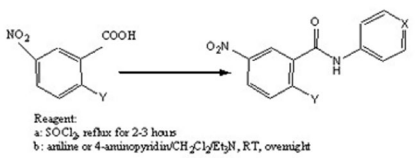

Table 1. List of 1st generation PPARγ antagonists

compound number	X	Y	EC_{50} (nM)
GW9662 (**2**)	C	Cl	13.9
1	C	Br	1.8
3	C	F	264.8
T0070907 (**5**)	N	Cl	148.3
4	N	Br	2.8
6	N	F	155.3

Keywords: PPAR gamma Antagonist, Biodistribution Study, In Vivo and In Vitro Study

16α-[^{18}F]FLUORO-17β-ESTRADIOL ([^{18}F]FES) BINDS LARGELY TO ESTROGEN RECEPTOR-α RECEPTORS

J. Yoo,[1] C.S. Dence,[1] T.L. Sharp,[1] J.A. Katzenellenbogen,[2] M.J. Welch.[1]
[1]Mallinckrodt Institute of Radiology, Washington University School of Medicine, St. Louis, MO, United States; [2]Department of Chemistry, University of Illinois, Urbana, IL, United States.

Tumors derived from estrogen target tissues, such as breast tumors, often have high levels of estrogen receptors, and assays of ER levels in tumors are used to assess the prospects for a favorable clinical response to hormonal therapy. Two estrogen receptor (ER) subtypes, ERα and ERβ, have rather different tissue distributions and different activity levels, and their response to estrogens of different structure can differ considerably.

We have attempted to determine the levels of both ERa and ERb in breast tumors by imaging. [^{18}F]FES is a well characterized ER imaging agent whose distribution pattern in other species, including

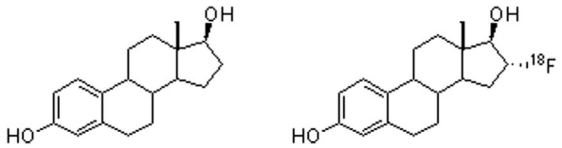

humans, had been well characterized. The relative binding affinity of FES was 55 with ERα and 22 with ERβ, giving a 2.5 fold preference for ERα (by definition, estradiol has a relative affinity of 100 for both ERs and hence no selectivity). Mice in which either ERα or ERβ was knocked out (αERKO and βERKO mice, respectively) were used as animal models to assess the dependence of radioligand uptake selectivity on ER subtype. As expected from its 2.5 fold ERα affinity selectivity, [^{18}F]FES uptake in βERKO mice (which have only ERa) was significantly higher than that in αERKO mice (which have only ERb) in all target organs. The highest %ID/g was observed in the uterus of diestrus βERKO mice at 30 min postinjection (18.9 ± 0.1 %ID/g). The βERKO/αERKO uterine and ovarian uptake ratios in animals increased with time, reaching maximum levels at 2 h (25.4 and 18.6, respectively). In contrast to comparable ovary uptakes in estrus (high estrogen) and non-estrus (low estrogen) mice, [^{18}F]FES uptake by the uterus of βERKO animals during estrus was 56% less than that during diestrus. In these different animal models, the patterns and time course of the tissue distribution of [^{18}F]FES are consistent with its high affinity and selectivity for ERα. Thus, [^{18}F]FES appears to function effectively as an imaging agent for ERα.

This work was supported by the United States Department of Energy (DEFG02-84ER-60218) and the National Institutes of Health (PHS 5R37 CA25836).

Keywords: Fluorine-18 Fluoroestradiol, Estrogen Receptor (ER), Knockout Mouse